METABOLIC PHENOTYPING USING KINETIC MEASUREMENTS IN HIGH- AND LOW-ACTIVE MICE

A Dissertation

by

JORGE GRANADOS

Submitted to the Office of Graduate and Professional Studies of
Texas A&M University
in partial fulfillment of the requirements for the degree of

DOCTOR OF PHILOSOPHY

Chair of Committee,	J. Timothy Lightfoot
Committee Members,	Roger Sansom
	James D. Fluckey
	Christopher R. Woodman
Head of Department,	Melinda Sheffield-Moore

December 2019

Major Subject: Kinesiology

ABSTRACT

Physical activity is well known to diminish the occurrence of many diseases, yet fewer than 10% of American adults adhere to recommended physical activity guidelines. Thus, there is a critical need to identify the biological mechanism(s) associated with the regulation of physical activity adherence. To better understand the mechanism(s) associated with regulating physical activity levels, we have extensively studied inbred mice previously classified as low-active (LA) or high-active (HA) and found several differentially expressed muscle and brain proteins that may be involved in metabolism. These proteomic findings suggest potential amino acid, metabolite, and enzymatic pathways, which may be associated with the differential physical activity levels in HA and LA mice.

As such, the purpose of this dissertation was to conduct an exploratory metabolic phenotyping assessment of amino acid kinetics in HA and LA mice. Methods consisted of administering a stable isotope tracer pulse cocktail containing several amino acids and metabolites. Subsequently, blood samples were collected at different time points (Time: 1, 3, 5, 7, 10, 15, 20, 25, 30, and 40 min) for liquid chromatography-tandem mass spectrometry assessment of plasma enrichments and concentrations of the infused tracers. Amino acid whole-body production and clearance were calculated.

This untargeted assessment identified differences in several amino acid pathways related to 1) modified arginine and nitric oxide production; 2) augmented energy flux via increased isoleucine and valine anaplerosis; 3) potential increases of dopamine *via*

increased phenylalanine and tyrosine metabolism. In conclusion, the observed differences in amino acid metabolism may be associated with the regulation of varying physical activity levels in HA and LA mice. Additionally, the identified metabolic pathways will serve as a foundation for follow-up intervention studies in the HA and LA mice.

DEDICATION

I dedicate this dissertation to my parents Eloisa and Hermilo Granados, and my brother Eduardo Granados. I couldn’t have made it this far without your continuous support.

ACKNOWLEDGEMENTS

I would like to express my earnest gratitude to my committee chair, Dr. Timothy Lightfoot, for providing me the opportunity to join his lab group four years ago. Thank you for your patience, guidance, leadership, hiking anecdotes, and for providing me with diverse opportunities for personal, scientific, and professional growth. Additionally, I'd like to thank the rest of my committee members, Dr. James D. Fluckey, Dr. Christopher R. Woodman, and Dr. Roger Sansom, for their guidance and support throughout the course of this research.

This dissertation is the culmination of the rigorous work invested by multiple scientists/colleagues. Primarily, I'd like to thank Dr. Nicolaas Deutz for welcoming me into his lab during the past two years and for his patience in guiding me through months of data processing, interpretation, and dissemination through written manuscripts. Moreover, a huge thank you to Dr. Gabrie Ten Have, for your continual mentorship and for teaching me the ins and out of developing a stable isotope tracer study, including the intricate mouse cannulation surgical procedures. Speaking of isotope tracers, thank you, Dr. John Thaden, for providing mass spectrometry expertise and for analyzing the hundreds of samples from this study. Also, I appreciate the work and time spent by current and past lab members (Dr. Ayland C. Letsinger, Chaz Nagel, Tatiana Padovani, Kat Stiegel, Jeremiah Velasco, Victor Garcia, Ben Nevares, and Leyla Perez) collecting blood and tissue samples during the surgery days and preparing those samples for mass spectrometry analysis.

Thanks also go to my friends and colleagues, department faculty, and the PEAP family for making my time at Texas A&M University a great experience. A special shout-out to my great friend and colleague, Dr. Ayland C Letsinger. Ayland, if I was given a choice to redo my doctorate journey and have my choice of a lab partner, I'd chose to do it all over again with you by my side. Dr. Tyler Grubic, thank you for sharing many long writing nights with me in the office, and for being by sparring/jiu-jitsu partner for the past three years. Dr. Boomer Trujillo, thank you from the bottom of my heart for always being by my side and supporting me thought the peaks and valleys of my doctoral experience. Kristina Cross, not sure if you're aware that my last year at Texas A&M, has been the best one yet because of you. Thank you for your constant love and encouragement.

I am very fortunate to have made lifelong friends and colleagues who have supported me in many ways thought these past five years; however, it would take many pages for me to thank everyone individually. For this reason, I'd like to give an enormous thank you to the following individuals: Dr. Heather Vellers, Ben Montemayor, Dr. Mathew Kuennen, Dr. Dustin Joubert, Dr. Chelsea Goodenough, Catherine Zabilski, Clayton Cruthirds, Agata McNew, Sarah Kirshner, Anna Salvador, Ryan Sowinski, Pat Ryan, Kalen Johnson, Faith Lightfoot, Dr. Robin Fuchs-Young, Javier Martinez, Patricio Reynaga, Navdeep Uppal and Johnny Hernandez. Know that whether big or small, you all have played a critical role in my journey and development, and for that, I am grateful.

Additionally, I'd like to thank Dr. Susan Bloomfield for nominating me to receive the Pathways to the Doctoral Fellowship. Dr. Crouse, thank you for bringing me onboard to the Applied Exercise Science Laboratory and allowing me to learn from you during my

initial year at Texas A&M. Dr. Bloomfield and Dr. Crouse, thank you once again, as I would literally not be here if it wasn't for you two. Lastly, thanks to my mother, Eloisa, and father Hermilo, and my brother Eduardo for their constant encouragement, patience, and love!

CONTRIBUTORS AND FUNDING SOURCES

Contributors

This work was supervised by a dissertation committee consisting of Professors J. Timothy Lightfoot [advisor], Christopher R. Woodman, and James D. Fluckey of the Department of Kinesiology and Professor Roger Sansom of the Department of Philosophy & Humanities.

The data analysis and interpretation for Chapter 2-4 were supervised by Professors Nicolaas Deutz, and Gabriella ten Have of the Department of Kinesiology. All liquid chromatography-mass spectrometry analysis was performed by Dr. John J. Thaden of the Department of Kinesiology. Sample collection and surgical procedures were a collaborative effort involving members from the Biology of Physical Activity Laboratory (Ayland C. Letsinger, Edward C. Nagle, Victor Garcia, Jeremiah Velasco, and J.Timothy Lightfoot) and the Center for Translational Research in Aging and Longevity (Gabriella ten Have, Nicolaas Deutz, Agata McNew, and Cristina Osorio)

All other work conducted for the dissertation was completed by the student independently.

Funding Sources

This dissertation was funded by a research development grant from the Vice-President of Research, Texas A&M University, and funding from the Omar Smith and Ponder endowments.

This work was also made possible by a Strategic Research Award Fellowship from the College of Education and Human Development, Texas A&M University, which provided me the time needed for data processing and analysis. The dissertation contents are solely the responsibility of the authors and do not necessarily represent the official views of any of the funding sources named above.

NOMENCLATURE

AA	Amino Acid
AUC	Area under the Curve
ARG	Arginine
ASL	Argininosuccinate lyase
ASS	Argininosuccinate synthase
BCAA	Sum of the Branched-Chain Amino Acids: Valine, Isoleucine, and Leucine
BCKA	Sum of the Branched-Chain Keto Acids: KIC, KIV, and KMV
BCKDH	Branched-Chain Alpha-Ketoacid Dehydrogenase
BP	Bound Protein
CIT	Citrulline
CVD	Cardiovascular Disease
DXA	Dual-Energy X-ray Absorptiometry
EAA	Sum of the Amino Acids: Threonine, Valine, Methionine, Isoleucine, Leucine, Tryptophan, Phenylalanine, Histidine and Lysine
EDTA	Ethylenediaminetetraacetic acid used as an anticoagulant
eNOS	Endothelial NO Synthase
FM	Fat Mass
FFM	Fat-Free Mass

GC/MS	Gas Chromatography-Mass Spectrometry
GLN	Glutamine
GLU	Glutamate
HFHS	High Fat High Sugar
HMB	β-Hydroxy β-Methylbutyrate
IC	Intracellular
IP	Intraperitoneal
ILE	Isoleucine
KIC	α-Ketoisocaproic Acid
KIV	α-Ketoisovalerate
KMV	α-Keto-β-Methylvalerate
LC-MS/MS	Liquid Chromatography-Tandem Mass Spectrometry
L-DOPA	L-3,4-Dihydroxyphenylalanine
LEU	Leucine
LNAA	Sum of the Amino Acids: Valine, Isoleucine, Leucine, Phenylalanine, and Tyrosine
LNAA/TRP	Ratio between the LNAA and Tryptophan concentration
NO	Nitric Oxide
NEAA	Sum of the Amino Acids: Aspartate, Glutamate, Asparagine, Glutamine, Serine, Glycine, Arginine, Alanine, Proline and Tyrosine
ORN	Ornithine

PHE	Phenylalanine
Ra	Rate of Appearance
TBV	Total Blood Volume
TTR	Tracer-Tracee Ratio
TYR	Tyrosine
TyrH	Tyrosine Hydroxylase
Tau-MetHis	Tau-Methyl-Histidine
VAL	Valine
WD	Western Diet
WBnetPB	Whole-body net Protein Breakdown
WBP	Whole-body Production
WbRa	Whole-body Rate of Appearance

TABLE OF CONTENTS

Page

ABSTRACT ii

DEDICATION iv

ACKNOWLEDGEMENTS v

CONTRIBUTORS AND FUNDING SOURCES viii

NOMENCLATURE x

TABLE OF CONTENTS xiii

LIST OF FIGURES xvi

LIST OF TABLES xvii

1. INTRODUCTION 1

1.1. High - and Low - Active Mouse Model 3
1.1.1. Protein Expression in High and Low Active Mice 4
1.2. Stable Tracer Pulse Methodology 5
1.3. Amino Acid Metabolism and Physical Activity 6
1.3.1. Arginine and the Nitic Oxide Pathway 7
1.3.2. Branched-Chain Amino Acids & Physical Activity 9
1.3.3. Phenylalanine and Tyrosine 11
1.4. Summary and Objective 12

2. ACTIVATED WHOLE-BODY ARGININE PATHWAY IN HIGH-ACTIVE MICE 13

2.1. Synopsis 13
2.2. Introduction 14
2.3. Materials and Methods 15
2.3.1. Animals 15
2.3.2. Study Protocol 16
2.3.3. Body Composition 17
2.3.4. Anesthesia Induction 17
2.3.5. Stable Tracer Infusion by IV Pulse 17
2.3.6. Sample Collection 18

2.3.7. Biochemical Analysis 18
2.3.8. Calculations 19
2.3.9. Statistical Analysis 20
2.4. Results 20
2.5. Discussion 22
2.5.1. Limitations 27

3. ELEVATED WHOLE-BODY PRODUCTION OF VALINE AND ISOLEUCINE IN HIGH-ACTIVE MICE 29

3.1. Synopsis 29
3.2. Introduction 30
3.3. Materials and Methods 31
3.3.1. Animals 31
3.3.2. Study Protocol 32
3.3.3. Body Composition 32
3.3.4. Anesthesia Induction 33
3.3.5. Stable Tracer Infusion by IV Pulse 33
3.3.6. Sample Collection 33
3.3.7. Biochemical Analysis 34
3.3.8. Calculations 34
3.3.9. Statistical Analysis 35
3.4. Results 35
3.5. Discussion 36
3.5.1. Does increased VAL and ILE stimulate anaplerosis? 36
3.5.2. BCAA in exercise and habitual Physical Activity 37
3.5.3. BCAA in Diabetes/Glucose Regulation 38
3.5.4. High-Active Animal Model 39
3.5.5. Conclusions 41

4. ELEVATED WHOLE-BODY PRODUCTION OF PHENYLALANINE AND TYROSINE IN HIGH-ACTIVE MICE 42

4.1. Introduction 42
4.2. Materials and Methods 43
4.2.1. Animals 43
4.2.2. Study Protocol 44
4.2.3. Body Composition 44
4.2.4. Anesthesia Induction 45
4.2.5. Stable Tracer Infusion by IV Pulse 45
4.2.6. Biochemical Analysis 46
4.2.7. Calculations 46
4.2.8. Statistical Analysis 47
4.3. Results 47

4.4. Discussion 48
4.4.1. Dopamine Production and Physical Activity 49
4.4.2. Can PHE and TYR Stimulate Anaplerosis? 49
4.4.3. Whole-Body Net Protein Breakdown and Tau-Methylhistidine 50
4.4.4. Conclusion 51

5. CONCLUSIONS 52

REFERENCES 54

APPENDIX A FIGURES 76

APPENDIX B TABLES 89

LIST OF FIGURES

Page

Figure 1: Study Timeline 76

Figure 2: Citrulline & Arginine Whole-Body Production 77

Figure 3: Whole-Body Production of ARG Metabolites 78

Figure 4: Nitric Oxide Production Ratio 79

Figure 5: Arginine Metabolic Pathway 80

Figure 6: TTR & Whole-Body Production of BCAA 81

Figure 7: BCAA Clearance Rates 82

Figure 8: Anaplerosis *via* Valine And Isoleucine 83

Figure 9: TTR & Whole-Body Production of Tau-Methyl-Histidine 84

Figure 10: Phenylalanine TTR & Whole-Body Production 85

Figure 11: Tyrosine TTR & Whole-Body Production 86

Figure 12: Clearance Rates of Phenylalanine, Tyrosine, & Tau-Methyl-Histidine 87

Figure 13: Anaplerosis *via* Phenylalanine & Tyrosine 88

LIST OF TABLES

Page

Table 1: Mouse Characteristics 89

Table 2: Plasma Amino Acid Concentrations 89

Table 3: Composition of Stable Tracers in Bolus Pulse 90

1. INTRODUCTION

Physical activity is known to diminish the occurrence of many diseases, such as type II diabetes (1-4) cardiovascular disease (CVD) (5-8), various cancers (9-12), and many other chronic conditions (13-18) . Physical inactivity in combination with poor diet accounts for 70% of deaths and is considered the second leading actual cause of death in the United States (19, 20). Additionally, hypokinetic related diseases resulted in an estimated global healthcare cost of $53.8 billion in 2013 (21). Despite the well-known benefits associated with moderate physical activity (22, 23), less than 10% of Americans over the age of 20 adhere to the recommended amount of weekly activity (i.e., 150 minutes per week of moderate-intensity) established by the American College of Sports Medicine (ACSM) (24). Moreover, Booth et al. reported that approximately 86% of the 325 million in the United States (U.S.) population achieve less than the U.S. Government and World Health Organization guidelines for daily physical activity for health (25). Thus, there is a critical need to identify the biological mechanism(s) associated with the regulation of physical activity adherence.

Given the detrimental implications associated with physical inactivity, its related chronic diseases and associated high healthcare costs, our laboratory's primary focus has been to identify and to understand the biological and genetic mechanisms that regulate physical activity with an end goal of developing potential countermeasures that may diminish and/or prevent the chronic diseases derived from physical inactivity. To establish a greater understanding of which mechanisms are associated with the regulation of

physical activity, our research studies have investigated a variety of different factors ranging from genetic and proteomic studies to pharmacological and exposure to environmental toxicants (26-43).

Although we have gained valuable knowledge along with a plethora of new research questions from our previous studies, it should be noted that all our studies have two commonalities: 1) they are all focused on physical activity and, 2) the results have all assumed that metabolism is similar between all experimental groups. Most recently, we performed a study to assess the effects of a high-fat high-sugar (HFHS) diet on wheel running and showed that exposure to HFHS diet severely decreased voluntary wheel running in males by 70 ± 28% and in females 57 ± 26% (44).

Interestingly, Meek et al. showed the opposite effects when mice selectively bred for high voluntary wheel running (HR mice) were exposed to a western-style diet (WD) with similar fat content (~42% total fat) to our HFHS study (45). Despite the WD significantly increasing both body mass and retroperitoneal fat pad mass, the HR mice, increased wheel running revolutions per day by up to 75%. The authors of this paper suggested the significantly increased wheel running observed in HR mice exposed to a WD may be caused by fuel usage during prolonged endurance exercise and direct behavioral effects on motivation. The contradictory results from our HFHS diet study and the WD study from Meek et al. suggested our previous assumption ─ that metabolism was similar between all experimental groups might not be accurate, giving rise to the question of how/which metabolic pathways may be associated with the potential regulation of differential physical activity levels.

To better assess this literature gap on metabolism and the potential regulation of physical activity levels, we collaborated with the Center for Translational Research in Aging and Longevity (CTRAL). This center/laboratory has many decades of experience investigating metabolic pathways (46-55) in both human and animal models. A collaborative study including CTRAL's metabolism expertise along with our experience investigating inbred mouse strains previously classified as high-active (HA [C57L/J]) and low-active (LA [C3H/HeJ]) (28-31, 33, 38, 56-59) would add to the existing body of knowledge regarding biological/genetic regulation of physical activity levels (60). Thus, we investigated how amino acid metabolic pathways differ between HA and LA mouse strains.

1.1. High - and Low - Active Mouse Model

Lightfoot et al. examined quantitative trait loci (QTL) along with physical activity measured via wheel running in 41 inbred mouse strains and found moderate to high heritability of physical activity (57). Our HA (C57/LJ) and LA (C3H/HeJ) models were derived from this and a previous 2008 study (43). Although there were other mouse strains with similar high (NOD/ShiLtJ and C57BR/CDJ) and low (WSB/EIJ and SJL/J) activity levels, the variability within the selected C57/LJ and C3H/HeJ was the lowest within each strain suggesting a more stable phenotype. Given the differences in high and low activity levels, our lab earlier compared the haplotype structure and expression profile in skeletal muscle and brain of our HA and LA mice models. Although expression of nine candidate genes was observed and single nucleotide polymorphisms (SNPs) were detected in regions of *Actn2, Casq1, Drd2, Lepr, and Papss2*, no SNPs associated with physical activity were

located in coding sequences or associated with any known regulatory sequences (33). This study concluded that genomic structural variation or gene expression data alone was not adequate to establish any of these genes' candidacy or causality with the regulation of physical activity.

1.1.1. Protein Expression in High and Low Active Mice

Despite the observed expression of candidate genes, it was necessary to investigate the protein expression in HA and LA mice, because gene expression does not necessarily indicate protein translation (61-63). Ferguson et al. (28) conducted proteomic studies that examined the differential protein expression in the nucleus accumbens ─ the brain region associated with the dopaminergic reward system ─ and the skeletal muscle of HA and LA mice (30). These two proteomic studies found nine differentially expressed proteins in the brain between HA and LA mice and noted that neural stress proteins and a protein linked with energy metabolism were associated with physical activity regulation in HA and LA mice (13). Further, when Ferguson and colleagues (15) assessed soleus and extensor digitorum longus muscle, they found proteins with higher expression patterns in the Krebs (TCA) cycle and calcium-regulating pathways (e.g., annexin A6 and calsequestrin 1) in HA mice while LA mice overexpressed proteins associated with cytoskeletal structure- and electron transport chain-related pathways (e.g., ATPase and NADH dehydrogenase). These proteomic results taken in conjunction with the earlier gene variant results suggested that there are potential amino acid, metabolite, and enzymatic pathways that may be associated with the differential activity levels in HA and LA mice.

1.2. Stable Tracer Pulse Methodology

The past decades have given rise to the use of stable, nonradioactive isotope tracers as a tool to probe the dynamics of specific metabolites (47). It is a standard method (50, 64, 65) for a single or mixture of multiple stable isotope tracers to be introduced intravenously into the circulatory systemic via a catheter placed in one arm or using a bolus injection. In human subjects, blood or other accessible tissues (e.g., muscle and adipose tissue) are collected from the other arm or thigh pre- and post-tracer infusion (66). In animal models, a similar infusion process occurs; however, more tissues are readily accessible for analysis (67). After injection, isotopic enrichment, defined as the "tracer" [or isotope infused] to "tracee" [or isotopes already in the body] ratio (*TTR*), in a tissue of interest, is then determined by utilizing gas chromatography-mass spectrometry (GC/MS) and or liquid chromatography-tandem mass spectrometry LC-MS/MS (68).

The next section focuses on the technicality of a single pulse of tracer (pulse) infusion delivery method and a more commonly used method known as primed-constant (PC) continuous infusion method. For a more detailed methodological review on the application of isotope tracers in metabolic research, see Kim et al. 2016 (66).

Although the PC method is commonly used for whole-body rate of amino acids (AA) appearance (WbR_a) in humans and animal models (67, 69, 70), this method usually focuses on using a compartmental model for WbR_a quantification. Therefore, we decided to use the pulse method, which utilizes a non-compartmental model, thus avoiding disadvantages which can occur when using the PC method such as needing prior knowledge of pool size to calculate isotope tracer priming doze or using large amounts of

stable tracers (49, 50, 67). When using the pulse approach, the shape of the TTR decay curve is dependent on the number of pools (e.g., organ tissues) connected to the extracellular (e.g., blood) pool. For most substrates like AA, the intracellular pool is the main secondary (e.g., muscle tissue) pool, and the amino acid decay curve reflects two compartments. This TTR decay curve can be used to implement both non-compartmental and compartmental modeling (71-73), thus allowing us to calculate the rate of appearance (R_a) into the extracellular and the intracellular pools, as well as the fluxes between the pools. Additionally, we can calculate the protein breakdown (PB) given the appearance of an essential amino acid (EAA) (e.g., phenylalanine) into the intracellular pool.

However, one disadvantage of utilizing the pulse method is the necessity to use more complex analysis calculations for quantification of the metabolites. Fortunately, there are well-established and validated computational (74, 75) and mathematical models (71, 76, 77) readily available, which allows for fitting and quantification of isotope tracers/metabolites. Moreover, the pulse method can be used to measure the flux between different metabolic routes (71, 78) and gives the ability to measure tissue-specific fractional protein synthesis rates (FSR) and fractional breakdown rates (FBR) (79-81).

1.3. Amino Acid Metabolism and Physical Activity

Given the many different metabolic pathways involved with amino acids and their role in physiological mechanisms regulating blood flow, energy production, and neurotransmitter activity, the next three sections focus on amino acids which have been investigated for exercise performance and could potentially be associated in the regulation of differential physical activity levels.

1.3.1. Arginine and the Nitic Oxide Pathway

Supplements that contain citrulline (CIT), arginine (ARG), or a combination of both have been heavily studied in the sports world as they are claimed to increase the production of nitric oxide (NO) (82-92). Despite the extensive ARG research, there are no specific nutritional requirements set for ARG in healthy adults, given that it is a conditionally EAA (93). Although the CIT to ARG pathway is involved in NO production, ergogenic supplement manufacturers continue to use misleading statements about NO creation. In the following sections, we describe how NO gained its popularity and discuss NO metabolic pathways and other essential roles of ARG and NO.

ARG was identified as the precursor for NO in the 1980s (94). In 1998, the Nobel Prize in Medicine was awarded to three American researchers (Robert F. Fruchgott, Louis J. Ignarro, and Ferid Murad) who discovered the vasodilator properties of NO. Although initially discovered in endothelial cells (95), NO appeared to be a ubiquitous molecule present in a variety of inflammatory and other cells, including cells from the nervous and cardiovascular systems.

As research progressed in this area, NO was found to have many physiological functions, and the relationship between ARG availability and NO production emphasized ARG's functional relevance. NO benefits the cardiovascular system by vascular muscle tone regulation (e.g., improved blood flow) and by reducing blood platelet adhesion (54, 95, 96). However, these benefits were said to be the cause of a synergistic effect between ARG (in a large enough dose) and CIT (89, 90, 97).

1.3.1.1. Arginine Metabolic Pathways

Dietary intake, body protein breakdown, or endogenous *de novo* ARG production are three different sources for ARG (54). In healthy adults, whole-body ARG flux is ~70–90 $\mu mol \cdot kg^{-1} \cdot h^{-1}$, equivalent to 15–20 g/day during the postabsorptive state (98), while daily dietary ARG intake is ~4–6 g (99, 100). Only 10–15% of whole-body ARG production is derived from *de novo* ARG production under normal conditions (101, 102). This pathway involves the conversion of CIT to ARG (CIT>>ARG) and is catalyzed by the enzymes argininosuccinate lyase (ASL) and argininosuccinate synthase (ASS) (103, 104). This conversion is part of the intestinal-renal axis, which involves intestinal production of CIT, while ARG is synthesized by the kidneys (105-107). Given this pathway, the limiting factor for this conversion to occur is CIT availability (104).

ARG is a crucial component for body protein synthesis, given that ~80% is derived from recycled AAs due to protein breakdown. Additionally, ARG is a crucial constituent in many metabolic pathways (108-110), and its metabolism is highly compartmentalized, given that enzymatic activity involved in ARG metabolism occurs in different organs (e.g., muscle and kidney). However, the compartmentalization causes ARG metabolism and recycling to be partly in balance with plasma ARG concentration. This imbalance is usually referred to as the "arginine paradox" and describes why acute exogenous ARG is able to increase NO production even though the intracellular ARG concentration far exceeds the K_m of endothelial NO synthase (eNOS) (91). There is a possibility that once ARG is transported into the cell, it fails to gain access to the membrane-bound eNOS, thus making intracellular ARG less useful as a reference point (111).

Additional roles of ARG are associated with metabolites derived from ARG. Roles such as the ARG conversion to ornithine (ORN) via the enzyme ORN aminotransferase can lead to increased CIT production (112). Proline (PRO), also derived from ARG by hydroxylation to hydroxyproline, has an essential role in collagen formation, tissue repair, and wound healing. Additionally, creatine, which plays a role in energy metabolism in muscles and neurons (110), is also a derivative of ARG. Interestingly, ARG is responsible for the activation of p70 S6 kinase and phosphorylation of 4E-BP1 through the mTOR signaling pathway (113) with stimulation of protein synthesis independent of NO (114). In conclusion, while ARG metabolic pathways pay may physiological roles, it is possible that ARG metabolism could potentially play a role in the regulation of physical activity levels.

1.3.2. Branched-Chain Amino Acids & Physical Activity

Branched-chained amino acid (BCAA) interventions for exercise performance has been a topic of high interest (115, 116). Currently, BCAA are a multimillion-dollar industry primarily because of the claim that consumption of dietary BCAA, specifically leucine (LEU), stimulates muscle protein synthesis, produces an anabolic response in human subjects, and provides anaplerotic benefits when valine (VAL) and isoleucine (ILE) are elevated (117). However, a 2017 review on the anabolic effects of BCAA concluded that the anabolic claim was unwarranted (118). A 2005 review (119) titled "Interrelationship Between Physical Activity and Branched-chain Amino Acids" mentioned PA in its title; however, it's only a review of BCAA and exercise and fails to

mention/assess interactions between endogenous BCAA metabolism and their relationship with inherent PA levels.

Recently, Xiao et al. (120) reported an untargeted metabolomics study considering 328 plasma metabolites in a group of 277 Chinese male and female adults. Xiao and colleagues showed 11 metabolites to be associated with a high level of physical activity energy expenditure. Interestingly, they observed that higher levels of PA were associated with lower plasma levels of VAL, ILE, and LEU metabolic pathways (120).

1.3.2.1. BCAA in Diabetes/Glucose Regulation

Recent BCAA studies have shifted focus towards BCAA metabolic association in fat metabolism (121-127), and within numerous systemic diseases (e.g., type 2 diabetes (T2D), cancer, and heart failure) (125, 128-131). For example, defects in mitochondrial β-oxidation and BCAA oxidation were associated with T2D and other conditions such as Huntington's disease and maple syrup urine (132-135). Because of these defective mitochondrial pathways, production of TCA cycle intermediates can be limited (136, 137), and obesity worsens the condition of the disease. Given the anaplerotic properties (i.e., replenishment process of depleted metabolic TCA cycle intermediates) of VAL and ILE (133, 134, 138, 139), these beta-oxidation malfunctions observed in obese T2D could hypothetically be restored.

The claim that VAL and ILE may serve in anaplerotic reactions within the TCA cycle is supported by a recent study (140) in which healthy mice selectively bred for high activity levels demonstrated increased PA levels when exposed to a WD (high-fat diet). It is possible that mice bred for high PA levels may be taking advantage of ILE's

anaplerotic properties given that ILE is both a glucogenic and ketogenic AA, thus increasing BCAA oxidation to propionyl-CoA in the blood and providing more ATP.

1.3.3. Phenylalanine and Tyrosine

We (38) and others have suggested (141-143) that the dopaminergic system may be responsible for the regulation of PA levels. More specifically, we have shown in HA and LA mice that genetic differences in dopamine signaling pathways may play a role in PA response to dopaminergic-acting drugs (56). Although the dopaminergic system is complex, dopamine biosynthesis can be affected by the availability of its precursor, L-3,4-dihydroxyphenylalanine (L-DOPA) (144), which is derived from tyrosine (TYR) through hydroxylation via the enzyme tyrosine hydroxylase (TyrH) (145). TYR is a non-essential amino acid, and it is primarily synthesized in the liver from the essential amino acid phenylalanine (PHE) through PHE hydroxylase (146). While PHE and TYR metabolism plays a key precursor role in dopamine production, these two AAs also play vital metabolic roles in energy production within the tricarboxylic acid cycle (TCA).

More precisely, after PHE is converted to TYR, a series of metabolic conversion steps occur and yield acetoacetate and fumarate, which can then be converted into a ketone body and glucose, respectively. Moreover, the total conversion of PHE to TYR can be utilized as a quantification for whole-body net protein breakdown. The quantification is important, as net protein breakdown can provide information on total protein recycling within the muscle and whole-body tissues.

1.4. Summary and Objective

Moderate physical activity (PA) reduces the occurrence of PA-related diseases such as type II diabetes, cardiovascular disease, and cancer; however, fewer than 10% of American adults older than 20 years of age engage in the recommended daily 30 min of moderate-intensity PA (24). With the detrimental implications associated with physical inactivity, its related chronic diseases, and the associated high healthcare costs, it is critical to understand biological factors that may play a role in regulating PA. Given the indirect evidence in the literature, it is possible that interactions between amino acid metabolic pathways exert potential regulatory roles in different PA levels.

The objective of this dissertation was to determine if amino acid metabolic pathways were associated with different physical activity levels. To fulfill our objective, we investigated the amino acid metabolism kinetics using a stable isotope tracer pulse to quantify amino acid plasma concentrations, whole-body production, and clearance fluxes in two inbred mouse models previously classified as either high-active (HA) or low-active (LA).

2. ACTIVATED WHOLE-BODY ARGININE PATHWAY IN HIGH-ACTIVE MICE

2.1. Synopsis

Physical inactivity-related diseases account for 70% of U.S. deaths and an estimated $54 billion in global healthcare costs, yet fewer than 10% of American adults adhere to recommended physical activity (PA) guidelines. Our previous studies suggest that endogenous metabolic mechanisms may be potentially regulating PA levels. One such metabolic mechanism is the vasodilatory roles of nitric oxide (NO) production via the precursor arginine (ARG) and ARG-related pathways. The purpose of this study was to assess ARG metabolism and its precursors [citrulline (CIT), glutamine (GLN), glutamate (GLU), ornithine (ORN), and phenylalanine (PHE)] by measuring plasma concentration and enrichments, whole-body production (WBP), *de novo* ARG and NO production, and clearance rates in mice previously classified as either low-active (LA) or high-active (HA). We assessed LA (n=23) and HA (n=20) male mice by administering a stable tracer pulse cocktail via jugular catheterization. Blood samples were measured for plasma enrichments via LC-MS/MS. WBP, clearance rates, and production of *de novo* ARG and NO were calculated. HA mice had lower plasma concentrations of GLU, CIT, and ORN, but no differences for GLN, PHE, and ARG. However, HA mice had higher estimated NO production, higher WBP for CIT, ARG, PHE, and lower GLU. No significant differences were observed in WBP for GLN, ORN, PHE, or *de novo* ARG. We concluded that HA

active mice have an activated whole-body ARG pathway, which may be associated with regulating PA levels via increased NO production.

2.2. Introduction

Physical inactivity-related diseases (e.g., type II diabetes, cardiovascular disease, and cancer (25)) accounted for 70% of U.S. deaths (147) and resulted in an estimated global healthcare cost of $53.8 billion in 2013 (21). Although moderate physical activity (PA) has been demonstrated to mitigate the incidence of physical inactivity-related diseases (22), fewer than 10% of Americans over the age of 20 adhere to recommended PA guidelines (150 minutes of moderate-intensity per week) (24).

To better understand the potential mechanism(s) regulating PA (voluntary wheel running) levels, we have studied inbred high-active (HA) and low-active (LA) mouse models (30, 33, 43, 57, 58, 148, 149). We recently found in HA mice that creatine kinase B and succinyl-CoA ligase are overexpressed in the nucleus accumbens of the brain (28). Because these two proteins are associated with endogenous metabolism (150), we hypothesize that endogenous metabolism may be involved in the regulation of PA levels.

While there are a variety of endogenous metabolic pathways that could be associated with the regulation of PA levels, we first wanted to study the nitric oxide (NO) precursor, arginine (ARG), and the ARG-related pathways because of NO's known roles in related circulatory pathways (85). ARG is a conditional essential amino acid (AA) in humans and is derived from 1) exogenous dietary intake (e.g., nuts, meat products, and nutritional supplements) and serves as a substitute for citrulline (CIT) synthesis through interorgan exchange of ornithine (ORN) conversion within the small intestine via arginase

II and ornithine transcarbamylase metabolic pathways (151, 152); 2) whole-body protein breakdown from muscle into phenylalanine (PHE) and glutamine (GLN) (54); and 3) via *de novo* ARG production within the intestinal-renal axis through CIT catalyzation by the enzymes argininosuccinate synthase and argininosuccinate lyase (54). ARG is used in many biological functions (108-110), including protein synthesis, creatine synthesis, and NO synthesis (92, 153-155).

Arginine's functions are known to be affected by exercise exposure, particularly the vasodilatory changes associated with NO production (82, 83, 156-158). Essentially, during PA (e.g., exercise), NO increases blood flow to muscles, thereby increasing delivery of nutrients and clearing of waste products, which may promote longer PA duration (159). We, therefore, hypothesize that NO derived from ARG may affect PA levels in mouse strains with different inherent PA levels.

To determine if metabolites of the ARG pathways were associated with the regulation of PA levels, we studied total AA concentrations. Additionally, we used a stable tracer approach to assess whole-body production (WBP), and clearance rates of ARG including metabolic precursors (GLN, glutamate (GLU), ornithine (ORN), CIT, and PHE) and products (*de novo* ARG and NO production) in HA and LA inbred mice in order to assess if differences in ARG metabolism were associated with inherent PA levels.

2.3. Materials and Methods

2.3.1. Animals

All procedures were approved by the institutional animal care and use committee (IACUC) of Texas A&M University. We assessed a total of 23 male C3H/HeJ mice

(inherently LA inbred strain) and 20 male C57L/J mice (inherently HA inbred strain). The inherent activity levels of these two strains are based on previous voluntary wheel running data (57). Mice were purchased from The Jackson Laboratory (Bar Harbor, ME, USA) at 10-weeks of age and group-housed in standard mouse-cages in light and temperature-controlled housing facility (12-hour light-dark cycle, room temperature 22-24°C). Water and a standard chow diet (Harlan Labs, Houston TX; 25.2% protein, 4.0 % fat, 39.5% carbohydrate, 3.3% crude fiber, 10% neutral fiber, and 9.9% ash) diet were provided *ad libitum.* After a two-week acclimation period, metabolic phenotyping procedures were performed via a terminal surgery. During the acclimation period, mice were not exposed to wheel-running activity for two reasons: 1) average PA levels of these two mouse strains have previously been described (57) (average wheel running distance: LA = 0.6 ± 1.1 km/day; HA = 9.5 ± 2.0 km/day); and 2) we have shown that multiple day exposure to running wheels can induce physiological changes due to exercise adaptation (33).

2.3.2. Study Protocol

Four hours before the commencement of surgical procedures, food was removed to study animals in a post-absorptive condition. Body composition was assessed post food removal, and mice were then placed in clean cages and left undisturbed until the start of surgical procedure (**Figure 1**). All metabolic testing was performed using a terminal surgical procedure adapted from Hallemeesch et al. (160), which consisted of sedating the animal and performing a jugular vein catheterization for delivery of isotope tracer bolus and sample collection (**Figure 1**). The study protocol was identical for both groups and lasted approximately 5.5 hours.

2.3.3. Body Composition

Bodyweight (bw) was assessed immediately after food withdrawal using a digital beam scale with lean body mass, fat mass, percent fat mass, total water, and free water measured via echo MRI (EchoMRI LLC, Houston, TX 77079; **Table 1**). Bone mineral density data were collected by dual-energy X-ray absorptiometry (DEXA [Lunar PIXImus densitometer, GE Lunar Corp. Fitchburg, WI]) while the animals were under anesthesia.

2.3.4. Anesthesia Induction

Mice were anesthetized via intraperitoneal (IP) injection (0.1 ml/10g body weight) containing a mixture of ketamine (1.25 mg/10g BW) and medetomidine (2 μg/10g BW) (160). Anesthesia was maintained using a continuous pump infusion of ketamine (0.35 mg/ 10 g bw/h) and medetomidine (0.35 μg/10g bw/h) at a rate of 0.1 ml/10 g bw/h, given subcutaneously (160). Fluid balance and blood pressure were maintained by an initial 1.5 ml IP saline injection (0.9% sterile, NaCl), and continuous pump infusion (Harvard PHD2000) of saline at a rate of 2.5 ml/hour delivered subcutaneously (160). Breathing was continuously monitored, and body temperature was monitored using a rectal thermistor and maintained at 37°C via heating pad and lamp.

2.3.5. Stable Tracer Infusion by IV Pulse

Under anesthesia, a peripheral catheter was placed in the right jugular vein for blood sampling and infusion of a stable isotope tracer pulse (0.1 ml; isotonic) containing L-(Guanidino-$^{15}N_2$)-ARG, L-(5-^{13}C; 4,4,5,5-D_4)-CIT, L- ($^{13}C_5$)-ORN, L-(1,2-$^{13}C_2$)-GLU, L-($^{15}N_2$)-GLN, and L-(Ring-$^{13}C_6$)-PHE (Cambridge Isotope Laboratories: Woburn, MA,

USA). The different concentrations (nmol/0.01 ml) for each tracer are as follows: ARG (381.7), CIT (137.2), ORN (245.9), GLN (1699.6), GLU (196.8), and PHE (271.8).

2.3.6. Sample Collection

Blood samples (0.05 - 0.1 ml per sample) were collected utilizing two sampling time schedules (schedule 1: t = 1, 5, 10, 20, and 30 minutes; schedule 2: t = 3, 7, 15, 25, and 40 minutes) after pulse administration (**Figure 1**). Mice were sampled according to schedule 1 or 2 in order to minimize the total volume of blood taken from each animal and to provide a wider range of temporal points for more accurate fitting of the resulting data. The volume of blood that was collected was replaced with an equal volume of sterile normal saline. In a preliminary study in which no tracer infusion occurred during the mouse surgery, we obtained blood samples to measure the background enrichment. After the cannulation and sampling procedure concluded, the animals were euthanized by removal of the heart. Venous lithium-heparinized blood was collected and immediately placed on ice. Within one hour, the blood samples were centrifuged (4 °C, 3120 x *g* for 5 min) to obtain plasma, which was then deproteinized with 0.1 vol of 33% (w/w) trichloroacetic acid and stored at −80 °C for later analysis of tracer enrichments and concentrations of AAs via liquid chromatography tandem-mass spectrometry (LC-MS/MS).

2.3.7. Biochemical Analysis

Plasma AAs and their tracer enrichments were measured batchwise with LC-MS/MS using procedures previously validated in our lab (49, 161-163). Isotope peak areas were automatically identified and integrated by the SignalFinder1 algorithm in

MultiQuant v. 3.0 (Sciex), exported to Excel for calculation of area ratios, and regressed using GraphPad Prism 8 as described in detail in our previous study (49)

2.3.8. Calculations

The decay (change over time) of the tracer/tracee ratio (TTR [injected stable tracers/naturally occurring AA being traced]) was group fitted with a two-exponential least-squares regression: TTR (t) = a*exp(−k1*t) + b*exp(−k2*t). The area under the curve (AUC) was calculated from the integral two exponential curves (76). Whole-body production (WBP) was then calculated as DOSE (amount of isotope tracer in the pulse)/AUC. Metabolites from the injected stable tracers were group fitted as TTR (t) = −a*exp(−k1*t) + b*exp(−k2*t), and the integral was calculated to represent the AUC.

We calculated the conversion of one AA into another AA by using the WBP of the product AA and the ratio between the AUC of the TTR from the pulse of the product/substrate (49). For example, the conversion of CIT to ARG (i.e., *de novo* ARG production) was calculated as WBP of ARG L-(Guanidino-$^{15}N_2$)-arginine * AUC-TTR (L- [5-^{13}C; 4,4,5,5-D_4]-arginine/AUC-TTR L- [5-^{13}C; 4,4,5,5-D_4]-CIT).

As the AUC calculation with the fitting procedure could not be done for the CIT metabolite tracer (*i.e.*, 06 CIT1 [Ureido-M1]) given that the 40-minute sampling procedure was insufficient to observe differences in the metabolite decay curve (**Figure 2-A**), based on our previously published work (160, 164-166) we performed an alternative calculation for NO production. As NO production = WBP(CIT) * AUC (06 CIT1 [Ureido-M1])/AUC(ARG2), it can also be re-written as NO production = WBP(CIT)/AUC(ARG2) * AUC (06 CIT1 [Ureido-M1]). We subsequently calculated the ratio between the

estimated NO production of HA and LA, assuming AUC (06 CIT1 [Ureido-M1]) was not different (**Figure 2-B**). The non-compartmental analysis was done using GraphPad Prism (version 8.1). Additionally, the clearance flux of the stable tracers was calculated as WBP/plasma concentration (67) and expressed as mL/min.

2.3.9. Statistical Analysis

Results are expressed as mean ± standard error (SE). If data failed normality or equal variance tests, they were log-transformed. Unpaired Student's *t*-tests were used to determine differences in body composition, plasma AA, and plasma metabolites between the HA and LA mouse groups. A one-sample Wilcoxon *t*-test with a hypothetical value of 1.0 was used to determine differences in NO production ratio. The statistical package within GraphPad Prism (Version 8.1) was used for data analysis. The level of significance was set *a priori* at $p < 0.05$.

2.4. Results

We analyzed a total of 43 male mice at twelve-weeks of age, 23 LA, and 20 HA (**Table 1**). Although no differences in total fat mass, bone mineral density, or average daily food consumption were observed, the HA mice were characterized by 6.7% higher total body weight ($p<0.0001$) due to a 6.4% higher lean mass ($p=0.0003$). The higher lean mass observed in the HA mice also explains the 7.0% higher total-body water observed in these mice. It should be noted that although the lean mass was higher in the HA mice, it only represents a 1.4 g difference in lean mass between HA and LA mice, thus suggesting that any differences observed in WBP and clearance rates could be associated with the difference in lean body mass. For this reason, we normalized our results to the animal's

lean body mass. The same statement can be applied to the total body water differences as they account for a 1.3 g difference between mouse strains.

Post-absorptive plasma concentrations of the six measured AAs are depicted in **Table 1**. Significantly lower concentrations were observed in the HA mice for GLU (71.1%, $p < 0.0001$), CIT (21.0%, $p = 0.0003$), and ORN (40.1%, $p = 0.0241$), while no significant differences were found in plasma concentrations for GLN, PHE, or ARG.

Despite lower concentrations of GLU, CIT, and ORN in the HA mice, we found that the HA mice had significantly higher WBP for CIT (21.8%, $p < 0.0001$; **Figure 3-A**), while having significantly lower WBP of GLU (78.5%; $p = 0.02$; **Figure 4-B**), with no difference in WBP for ORN ($p=0.17$; **Figure 4-C**). Additionally, despite no differences in the concentrations of GLN, PHE, or ARG, the HA mice had significantly higher WBP ARG (21.4%, $p < 0.0001$; **Figure 3-B**), and PHE (7.6%, $p < 0.01$; **Figure 4-A**), while having no differences in the WBP of GLN ($p = 0.51$; **Figure 4-D**). Additionally, we found no differences in the conversion of CIT to ARG (i.e., *de novo* ARG production between the LA and HA mice (0.83 ± 0.05 vs. 0.92 ± 0.07 nmol/g lbm/min; $p = 0.28$).

There were no differences ($p = 0.15$) during the 40-minute decay curve for the metabolite 06 CIT1 [Ureido-M1] between the groups **(Figure 2-A)**. We then calculated the ratio between LA and HA and found that the ratio between the estimated NO production was 0.64 ± 0.08 ($p = 0.0197$; **Figure 2-B)**. Therefore, the ratio between estimated NO production was lower in LA mice, suggesting HA mice had higher NO production.

With the measurement of AA plasma concentrations and WBP, we calculated the AA clearance rates. We found the HA group had a 42.3% increased clearance rate for CIT, 19.5% for ARG, and 48.4% for ORN and 18.5% for PHE (all p values < 0.0001) compared to the LA group (**Table 1**). There was no significant difference in clearance rates for GLN (5.3%, p = 0.25) or GLU (8.6%, p = 0.33) in HA mice compared to LA mice (**Table 1**).

2.5. Discussion

Our purpose was to determine if endogenous metabolic pathways could be associated with physical activity levels. Overall, our data suggest HA mice have modified ARG and related pathways that were associated with their high PA levels. The modification of the ARG pathways includes both alterations in whole-body production and clearance of various AA, which appear to lead to differential NO responses in high active mice.

We observed HA mice have higher WBP (**Figure 2-B**) and clearance (**Table 1**) of ARG with no resulting overall change in plasma concentrations (**Table 1**) compared to LA mice. Despite the HA mice showing higher WBP and clearance capacity of ARG, the lack of change in ARG plasma concentrations between mouse strains can be explained by the high compartmentalization and recycling of ARG within various body organs (54). For example, the liver produces ARG via the complete urea cycle but does not release ARG into plasma, thus not contributing to total ARG plasma concentrations (110). However, given the compartmentalization of ARG metabolism, alterations in WBP and clearance of ARG may represent other factors that affect endogenous metabolic pathways.

For example, it is possible that strain differences, weight, activity exposure, or diet, could have affected ARG metabolism differentially between the strains.

The basis for the difference between inbred strains is the underlying genomic variations between these strains. We have studied these two strains' genomic and proteomic profiles extensively in the past (28, 29, 43, 58, 148) to understand the underlying genomic/proteomic factors that differentially regulate the physical activity levels of these two strains. We found potential proteomic differences in the past (28) that may provide the underlying genomic mechanisms that control the observations we have made. Such proteomic differences include overexpression of succinyl CoA ligase and cluster of creatine kinase B in the nucleus accumbens-brain region that plays a central role in the reward circuit. Interestingly, both succinyl CoA ligase and creatine kinase B are involved in energy metabolism. Primarily, succinyl CoA ligase accelerates the transduction of the intermediate succinyl CoA into the citric acid cycle, and creatine kinase B plays an essential catalytic role in the transfer of phosphate between ATP and several phosphagens within tissues that have significant fluctuating energy demands (e.g., brain, skeletal muscle, heart, and liver).

Moreover, the gene responsible for the metabolic pathway of creatine kinase B is located in chromosome 12 (location: 111669355–111672338) (57), near a single nucleotide polymorphism associated with the regulation of PA distance (location: 89,352,286) (148). Given that ARG is needed for creatine synthesis (167), creatine is utilized during energy transduction reactions, and our previous study showing overexpression of creatine kinase B in the nucleus accumbens (28), it can be speculated

that higher WBP of ARG found in HA mice serves to provide higher energy transduction within skeletal muscle which could be related to their higher PA levels. Therefore, it is probable the differential genomic structure of the HA and LA mice contributed to the differential ARG metabolism observed in this study, a finding that validates using a genomically-controlled model such as inbred mice (versus outbred mice) to explore differential pathways that are associated with physical activity.

Other external factors that could have influenced ARG metabolism pathways were controlled for during this study. As a control for aging effects, both mouse groups were analyzed at 12-weeks of age (peak physically active age for most mice (149)). Additionally, while the HA group had a 6.4% higher lean mass than the LA mice, which was different from our earlier results (57), we controlled for these mass differences by standardizing our results by lean body mass. To prevent potential training-induced changes in metabolism, we studied naive animals (i.e., not exposed to a running wheel) given we have previously shown running wheel exposure can affect gene expression (33). Lastly, as a check on potential diet-induced changes in metabolism, both strains had the same daily average food consumption, which controlled for potential differences in metabolism induced by varying caloric intake composition or volume (**Table 1**). Therefore, other than known genomic differences that have been associated with physical activity regulation, we conclude the animals studied were not exposed to other external factors that would have altered ARG metabolism.

Without external factors altering ARG metabolism, differences in ARG metabolism should be a result of alterations in various endogenous factors. Because ARG

can be derived from whole-body protein breakdown, dietary intake, and *de novo* production via the intestinal-renal axis (53, 54), we assessed if endogenous factors contributed to the observed WBP of ARG in HA mice. This assessment was supported by two factors: First, given that PHE is a proxy for measuring whole-body protein breakdown (76, 77), the observed higher WBP of PHE suggests that HA mice have higher rates of protein breakdown, which contribute to the higher WBP of ARG. Secondly, because plasma concentrations are associated with the disposal capacity of their corresponding substrates (168), our findings suggest that although the observed lower PHE plasma concentrations were only trending to be significantly lower ($p=0.07$) in the HA mice, this observed lower trend is due to increased clearance rates for PHE. Thus, whole-body protein breakdown and higher clearance capacity of PHE were contributing to the higher WBP of ARG in HA mice independent of exogenous ARG intake (given that diet was controlled).

Another potential source of an increased ARG WBP is through the intestinal-renal axis and the *de novo* ARG production pathways. In order to assess if the higher WBP of ARG is derived from the intestinal-renal axis pathway (**Figure 5**), we assessed plasma concentrations (**Table 1**), WBP (**Figure 2 & 3**), and clearance fluxes (**Table 1**) of CIT, its precursors (GLN, GLU, ORN), and the conversion product of CIT to ARG (i.e., *de novo* ARG) (169). We found no differences in GLN plasma concentrations, WBP, or clearance rates between strains, suggesting muscle protein breakdown and resynthesis of GLN in the small intestine is constant, and therefore, not affecting GLN as a precursor for CIT production. Additionally, we observed significantly lower plasma concentrations and

WBP of GLU in the HA mice without a difference in GLU clearance rate. This observation suggests the lower GLU WBP was potentially due to GLU being utilized in other metabolic pathways outside of the small intestine, and thus not contributing to the WBP of ORN or CIT. The mechanisms responsible for reduced GLU concentrations in the HA animals may include neuronal excitability, synaptic plasticity, immunity, and behavior within the central nervous system (170); however, we suggest GLU in HA mice is potentially being utilized in an anaplerotic reaction as a substrate to replenish the TCA-Cycle intermediate 2-oxoglutarate when this intermediate is being extracted for biosynthesis. Also, despite ORN WBP not being different between strains, total plasma concentration was lower, and the clearance rate for ORN was higher in HA mice. This reduction of ORN plasma concentration and increased clearance rate suggest HA mice utilize these AAs at a faster rate than LA mice, which may be related to their higher PA levels. Lastly, we observed decreased CIT plasma concentrations along with an increase in CIT WBP and clearance rate. These observations suggest more CIT is being produced in the small intestine independent of the AA intestinal precursors (i.e., GLN, GLU, ORN) and utilized within the kidney for production of ARG (i.e., *de novo* ARG). However, despite the calculated *de novo* ARG WBP being 10.3% greater in HA mice, this difference was not statistically significant. Therefore, increased WBP and clearance of CIT independent of its precursors and the lack of WBP change in *de novo* ARG suggest the intestinal-renal axis pathway is not responsible for the elevated WBP of ARG in HA mice.

Although ARG is a versatile AA with multiple metabolic fates (e.g., synthesis of protein, creatine, polyamines, agmatine, urea (109)), we hypothesize the higher WBP and

clearance of ARG observed were related to higher production of NO which influenced the high activity level of these mice. We base this hypothesis on two observations. First, the combined WBP levels of CIT and PHE contributed a 21.4% higher ARG WBP in HA mice. Secondly, the observed higher ratio utilized as a proxy for NO production (**Figure 2-B**) in HA mice suggests these mice may have a higher production of NO (**Figure 5**). Therefore, a higher NO production would increase vasodilation, providing HA mice with increased blood flow, nutrient delivery, and waste removal in the working tissues (e.g., muscles). Consequently, the elevated ARG pathway presents itself as a metabolic mechanism which in theory, could influence the PA levels of HA mice.

In conclusion, the decreased CIT and PHE plasma concentrations, the higher CIT and PHE contribution to higher ARG WBP, the higher estimated NO production ratio, and the increased clearance rates for CIT, PHE, and ARG observed in HA mice, suggested an activated ARG pathway in those mice that were inherently more physically active. Moreover, the higher ratio for estimation of NO production in HA mice shows the activated ARG pathway may serve as a precursor to increasing NO production, which may be potentially linked to their exhibition of higher PA levels.

2.5.1. Limitations

It should be noted that the WBP values reported in this study are ~ four-fold higher than what we have previously reported in other studies (160, 171-174). Our previous rodent studies used primed-constant infusion protocols, which can cause an underestimation of GLN, given that GLN has a considerably large pool size (175).

However, the present study used a single pulse approach, which we expected to provide us with higher values that are probably less than that of the actual values (49, 50).

Moreover, despite our efforts to prevent potential training-induced changes in metabolism by studying naive animals (i.e., not exposed to a running wheel), it is possible that differences in daily cage ambulation could have altered metabolic pathways. However, we have previously shown that running wheel measures of activity do not correlate with measures of daily cage ambulation (57). Another limitation is that from this data alone, we cannot conclude that the observed differences are not due to mouse strain differences or PA disposition.

3. ELEVATED WHOLE-BODY PRODUCTION OF VALINE AND ISOLEUCINE IN HIGH-ACTIVE MICE

3.1. Synopsis

The essential amino acids, valine (VAL), isoleucine (ILE), and leucine (LEU) – known as the branched-chain amino acids (BCAA) have been studied for muscle wasting disorders and within numerous systemic diseases (e.g., diabetes, cancer, and heart failure). However, little is known about the metabolic interactions between BCAA and the potential regulation of physical activity (PA) levels. Our previous study suggests that endogenous metabolic mechanisms are potentially regulating PA levels. One such metabolic mechanism involves the anaplerotic reactions which replenish the TCA cycle intermediate succinyl-CoA *via* succinate ligase production *via* the precursors ILE and VAL. We assessed the metabolism of BCAA by measuring plasma concentration and enrichments, whole-body production (WBP), and clearance rates in mice previously classified as either low-active (LA) or high-active (HA). Under anesthesia, we assessed LA and HA male mice by administering a pulse cocktail containing BCAA stable tracers via jugular catheterization. BCAA WBP and clearance rates were calculated. HA mice have lower plasma concentrations of LEU ($p=0.0184$), ILE ($p=0.0041$), and VAL ($p=0.0008$), as well as lower clearance rates for all BCAA ($p>0.0001$). WBP in HA was only higher for ILE ($p=0.0189$) and VAL ($p=0.0019$). In conclusion, the stimulated VAL and ILE whole-body utilization and clearance pathways observed in HA mice could lead to improved anaplerotic reactions.

3.2. Introduction

For several decades, the essential amino acids valine (VAL), isoleucine (ILE), and leucine (LEU) – known as the branched-chain amino acids (BCAA) have been extensively studied for their roles in exercise performance (115, 116, 176-190) and protein synthesis (191-201). However, these exercise and protein synthesis studies have primarily focused on the performance-enhancing qualities derived from VAL, ILE, and LEU supplementation and have not assessed the metabolic interactions between BCAA and the potential regulation on physical activity (PA) levels. A better understanding of the BCAAs' metabolic interactions with PA levels is of crucial importance given that moderate PA is associated with the diminished prevalence of diseases (22, 25) and their causal economic burden on healthcare costs (21). Despite the known health benefits of PA, the percentage of American adults who adhere to the recommended PA guidelines (i.e., 150 minutes of moderate-intensity per week) is less than 10% (24).

Unlike LEU, VAL and ILE can undergo anaplerotic (re-filling) reactions within the tricarboxylic acid cycle (TCA)(202). When TCA intermediates such as succinyl-coenzyme-A (succinyl-Co-A) are diverted due to disease conditions (e.g., Type II Diabetes), the energy cycle is broken, and can no longer function properly. Essential energy production is resumed when the diverted intermediate(s) can be replenished by anaplerotic reactions (203, 204) ─ a process also known as anaplerosis (202).

After VAL and ILE are oxidized in the mitochondrial matrix, they undergo anaplerosis as they enter the TCA cycle through succinyl-CoA via propionyl-CoA and methylmalonyl-CoA (205). Succinyl-CoA is then converted to succinate and free CoA via the TCA enzyme succinyl-CoA ligase, also known as succinate synthase (150). Additionally,

succinyl-CoA ligase is responsible for energy production by converting guanosine diphosphate (GDP) to guanosine triphosphate (GTP) or adenosine diphosphate (ADP) to adenosine triphosphate (ATP) (206, 207).

To better understand the potential mechanism(s) regulating PA levels, we have studied inbred mouse strains previously classified to be high-active (HA), and low-active (LA) mouse models (30, 33, 43, 57, 58, 148, 149). We showed (28) that HA mice have overexpression of succinyl-CoA ligase in the nucleus accumbens ─ a brain region associated with the regulation of PA (29, 42, 143, 208). Given the observed overexpression of succinyl-CoA ligase in the nucleus accumbens of the HA mouse brain (28), VAL and ILE's anaplerotic properties within the TCA intermediate succinyl-CoA, and data depicting PA alterations in mice exposed to different glucogenic and ketogenic diets (44, 45, 209), we hypothesize that endogenous BCAA metabolism may be involved with the regulation of PA levels. To determine if differences in BCAA metabolism were associated with the regulation of inherent PA levels, we studied total AA concentrations and used a stable tracer approach to assess whole-body production (WBP), and clearance rates of VAL, ILE, and LEU in HA and LA inbred mice.

3.3. Materials and Methods

3.3.1. Animals

All procedures were approved by the institutional animal care and use committee (IACUC) of Texas A&M University. We assessed a total of 23 male C3H/HeJ mice (inherently LA inbred strain) and 20 male C57L/J mice (inherently HA inbred strain). The characteristic activity levels of these two strains are based on previous voluntary wheel running data (42) with these strains used in several subsequent studies (28-31, 33, 56, 208).

Mice were purchased from The Jackson Laboratory (Bar Harbor, ME, USA) at 10-weeks of age and group-housed in standard mouse-cages in light and temperature-controlled housing facility (12-hour light-dark cycle, room temperature 22-24°C). Water and a standard chow diet (Harlan Labs, Houston TX; 25.2% protein, 4.0 % fat, 39.5% carbohydrate, 3.3% crude fiber, 10% neutral fiber, and 9.9% ash) diet were provided *ad libitum.* After a two-week acclimation period, metabolic phenotyping procedures were performed via a terminal surgery. During the acclimation period, mice were not exposed to wheel-running activity for two reasons: 1) average PA levels of these two mouse strains have previously been described (57) (average wheel running distance: LA = 0.6 ± 1.1 km/day; HA = 9.5 ± 2.0 km/day); and 2) we have shown that multiple day exposure to running wheels can induce physiological changes due to exercise adaptation (33).

3.3.2. Study Protocol

Four hours before the commencement of surgical procedures, food was removed to study animals in a post-absorptive condition. Body composition was assessed post food removal, and mice were then placed in clean cages and left undisturbed until the start of surgical procedure (**Figure 1**). All metabolic testing was performed using a terminal surgical procedure adapted from Hallemeesch et al. (160), which consisted of sedating the animal and performing a jugular vein catheterization for delivery of isotope tracer bolus and sample collection (**Figure 1**). The study protocol was identical for both groups and lasted approximately 5.5 hours.

3.3.3. Body Composition

Bodyweight (bw) was assessed immediately after food withdrawal using a digital beam scale with lean body mass, fat mass, percent fat mass, total water, and free water

measured via echo MRI (EchoMRI LLC, Houston, TX 77079; **Table 1**). Bone mineral density data were collected by dual-energy X-ray absorptiometry (DEXA [Lunar PIXImus densitometer, GE Lunar Corp. Fitchburg, WI]) while the animals were under anesthesia.

3.3.4. Anesthesia Induction

Mice were anesthetized via intraperitoneal (IP) injection (0.1 ml/10g body weight) containing a mixture of ketamine (1.25 mg/10g BW) and medetomidine (2 μg/10g BW) (160). Anesthesia was maintained using a continuous pump infusion of ketamine (0.35 mg/ 10 g bw/h) and medetomidine (0.35 μg/10g bw/h) at a rate of 0.1 ml/10 g bw/h, given subcutaneously (160). Fluid balance and blood pressure were maintained by an initial 1.5 ml IP saline injection (0.9% sterile, NaCl), and by continuous pump infusion (Harvard PHD2000) of saline at a rate of 2.5 ml/hour delivered subcutaneously (160). Breathing was continuously monitored, and body temperature was monitored using a rectal thermistor and maintained at 37°C via a heating pad and lamp.

3.3.5. Stable Tracer Infusion by IV Pulse

Under anesthesia, a peripheral catheter was placed in the right jugular vein for blood sampling and infusion of a stable isotope tracer pulse (0.1 ml; isotonic) containing L- ($^{13}C_6$)-LEU, L-(1-^{13}C)-ILE, and L-($^{13}C_5$)-VAL (Cambridge Isotope Laboratories: Woburn, MA, USA). The different concentrations (nmol/0.01 ml) for each tracer are as follows: LEU (474.4), ILE (395.4), and VAL (993.1).

3.3.6. Sample Collection

Blood samples (0.05- 0.1 ml per sample) were collected utilizing two sampling time schedules (schedule 1: t = 1, 5, 10, 20, and 30 minutes; schedule 2: t = 3, 7, 15, 25, and 40 minutes) after pulse administration (**Figure 1**). Mice were sampled according to schedule 1

or 2 in order to minimize the total volume of blood taken from each animal and to provide a wider range of temporal points for more accurate fitting of the resulting data. The volume of blood that was collected was replaced with an equal volume of sterile normal saline. In a preliminary study in which no tracer infusion occurred during the mouse surgery, we obtained blood samples to measure the background enrichment. After the cannulation and sampling procedure concluded, the animals were euthanized by removal of the heart. Venous lithium-heparinized blood was collected and immediately placed on ice. Within one hour, the blood samples were centrifuged (4 °C, 3120 x *g* for 5 min) to obtain plasma, which was then deproteinized with 0.1 vol of 33% (w/w) trichloroacetic acid and stored at −80 °C for later analysis of tracer enrichments and concentrations of AAs via liquid chromatography tandem-mass spectrometry (LC-MS/MS).

3.3.7. Biochemical Analysis

Plasma AAs and their tracer enrichments were measured batchwise with LC-MS/MS using procedures previously validated in our lab (49, 161-163). Isotope peak areas were automatically identified and integrated by the SignalFinder1 algorithm in MultiQuant v. 3.0 (Sciex), exported to Excel for calculation of area ratios, and regressed using GraphPad Prism 8 as described in detail in our previous study (49).

3.3.8. Calculations

The decay (change over time) of the tracer/tracee ratio (TTR [injected stable tracers/naturally occurring AA being traced]) was group fitted with a two-exponential least-squares regression: $TTR(t) = a*\exp(-k1*t) + b*\exp(-k2*t)$. The area under the curve (AUC) was calculated from the integral two exponential curves (76). Whole-body production (WBP) was then calculated as DOSE (amount of isotope tracer in the

pulse)/AUC. Metabolites from the injected stable tracers were group fitted as TTR (t) = −a*exp(−k1*t) + b*exp(−k2*t), and the integral was calculated to represent the AUC. The non-compartmental analysis was done using GraphPad Prism (version 8.1). Additionally, the clearance flux of the stable tracers was calculated as WBP/plasma concentration (67)and expressed as mL/min.

3.3.9. Statistical Analysis

Results are expressed as mean ± standard error (SE). If data failed normality or equal variance tests, they were log-transformed. Unpaired Student's *t*-tests were used to determine differences in body composition, plasma AA, and plasma metabolites between the HA and LA mouse groups. A one-sample Wilcoxon *t*-test with a hypothetical value of 1.0 was used to determine differences in NO production ratio. The statistical package within GraphPad Prism (Version 8.1) was used for data analysis. The level of significance was set *a priori* at $p < 0.05$.

3.4. Results

We analyzed a total of 43 male mice at twelve-weeks of age, 20 HA, and 23 LA (**Table 1**). Although no differences in total fat mass, bone mineral density, or average daily food consumption were observed, the HA mice were characterized by 6.7% higher total body weight ($p<0.0001$) due to a 6.4% higher lean mass ($p=0.0003$). The higher lean mass observed in the HA mice also explained the 7.0% higher total-body water observed in these mice. It should be noted that although the lean mass was higher in the HA mice, it only represented a 1.4 g difference in lean mass between HA and LA mice, thus suggesting that any differences observed in WBP and clearance rates could be associated with the difference in lean body mass. For this reason, we normalized our results to the animal's lean body mass.

We applied a similar rationale to the total body water differences as they accounted for a 1.3 g difference between mouse strains.

In addition to the mouse characteristics, **Table 1** also depicts post-absorptive plasma concentrations of BCAA. Significantly lower concentrations were observed in the HA mice for all BCAA ─ VAL (18%, $p = 0.0008$), ILE (17.3%, $p = 0.0041$), and LEU (14.5%, $p = 0.0184$). Despite lower concentrations of all three BCAA in the HA mice, we found that the HA mice had significantly higher WBP for VAL (18.2%, $p < 0.0019$; **Figure 6-A**), and for ILE (33.2%, $p < 0.0189$; **Figure 6-B**). No significant differences in WBP for LEU (3.8%; $p = 0.5592$; **Figure 6-C**) were observed. We calculated the BCAA clearance rates from the measurement of AA plasma concentrations and WBP. We found the HA group had a 36.0% increased clearance rate for VAL, 49.8% for ILE, and 18.2% for LEU (all p values < 0.0001) compared to the LA group (**Figure 7 A-C**).

3.5. Discussion

Our purpose was to determine if endogenous BCAA metabolic pathways were associated with physical activity levels. Overall, our data suggest HA mice have stimulated VAL and ILE related pathways that were associated with their high PA levels. The modification of these pathways includes both alterations in whole-body production and clearance, while LEU only showed alterations in total clearance. These VAL and ILE stimulated pathways could lead to improved anaplerotic reactions in the high active mice, which may be associated with their inherently high PA levels.

3.5.1. Does increased VAL and ILE stimulate anaplerosis?

During homeostasis, increased VAL and ILE can stimulate anaplerosis (202). These anaplerotic stimulations occur in VAL and ILE, but not in LEU due to the differences in

glucogenic and ketogenic properties. VAL is a considered a glucogenic AA, LEU is a ketogenic AA, whereas ILE is considered both; thus, these BCAA undergo different catabolic reactions after entering the mitochondrial matrix (204). For instance, when VAL, ILE, and LEU enter skeletal muscle cells, they are first transaminated by branched-chain aminotransferase (BCAT) into the branched-chain keto acids (BCKA) α-keto-isovalerate (KIV), α-keto-b-methylvalerate (KMV), and α-ketoisocaproate (KIC) respectively.

Transamination by BCAT into BCKA is followed by an irreversible catabolic step (210) driven by the Branched-Chain Alpha-Ketoacid Dehydrogenase (BCKDH) complex in which KIV and KMV undergo several reactions to form propionyl-CoA, and KIC forms acetoacetate (123). LEU's BCKA product ─ acetoacetate ─ undergoes several steps to produce acetyl-CoA (211); however, this process does not promote anaplerosis given that acetyl-CoA needs several other intermediate steps before the potential to stimulate mitochondrial energetic flux. The VAL and ILE BCKAs product ─ Propionyl-CoA ─ reacts with Biotin to produce methylmalonyl-CoA, which is then acted on by the enzyme methylmalonyl-CoA Mutase to enter the TCA cycle as the intermediate Succinyl-CoA (205). Therefore, increased VAL and ILE transamination can promote anaplerosis and stimulate mitochondrial energetic flux.

3.5.2. BCAA in exercise and habitual Physical Activity

Since the late 1980s, BCAA interventions for exercise performance has been a topic of interest (115, 116). Today, BCAA are a multimillion-dollar industry primarily because of the claim that consumption of dietary BCAA (specifically LEU) stimulates muscle protein synthesis or produce an anabolic response in human subjects, and the anaplerotic benefits provided when VAL and ILE are elevated(117). However, a recent 2017 review on the

anabolic effects of BCAA concluded that the anabolic claim was unwarranted (118). A 2005 review (119) titled "Interrelationship Between Physical Activity and Branched-chain Amino Acids" mentioned PA in its title; however, it's only a review of BCAA and exercise and (212) fails to mention/assess interactions between endogenous BCAA metabolism and their relationship with innate PA levels.

Recently, Xiao et al. (120) reported their findings from an untargeted metabolomics study where they examined 328 plasma metabolites in a group of 277 Chinese male and female adults. Subsequently, Xiao and colleagues showed 11 metabolites to be associated with a high level of physical activity energy expenditure. Interestingly, they observed that a higher level of PA is associated with lower plasma levels of VAL, ILE, and LEU and of carbohydrates in metabolic pathways (120).

The reported BCAA plasma levels associated with higher PA levels in adults coincide with our current findings of lower VAL, ILE, and LEU plasma concentrations in HA mice (**Table 2**). The lower plasma concentrations shown in HA mice along with their higher clearance rates for all BCAA (**Figure 7 A-B**) suggest that HA mice have an increased turnover for VAL, ILE, and LEU. However, VAL and ILE were the only two AAs depicting a higher WBP (**Figure 6-A & B**). These WBP observations suggest HA mice have higher oxidation of VAL and ILE to propionyl-CoA and methylmalonyl-CoA and increasing the TCA intermediate Succinyl-CoA, thus promoting anaplerosis and stimulating mitochondrial energetic flux.

3.5.3. BCAA in Diabetes/Glucose Regulation

Recent BCAA studies have shifted focus towards BCAA metabolic association in fat metabolism (121-127), and within numerous systemic diseases (e.g., type 2 diabetes (T2D),

cancer, and heart failure) (125, 128-131). For example, defects in mitochondrial β-oxidation and BCAA oxidation are associated with T2D and other conditions such as Huntington's disease and maple syrup urine disease (132-135). Because of these defective mitochondrial pathways, the production of TCA cycle intermediates can be limited (136, 137), and obesity worsens the condition of the disease. Based on our VAL and ILE observations, these beta-oxidation malfunctions observed in obese T2D could hypothetically be restored by replenishing the depleted TCA cycle intermediates via anaplerotic reactions.

This anaplerotic claim is supported by a recent study (140) in which healthy mice selectively bred for high activity levels demonstrated an increase in their PA levels when exposed to a WD (high-fat diet). Since we didn't observe any changes in LEU WBP in our inbred HA mice **(Figure 6-C**), we hypothesize that mice selectively bred for high PA levels may be taking advantage of ILE's anaplerotic properties given that ILE is both a glucogenic and ketogenic amino acid, thus increasing BCAA oxidation to propionyl-CoA in the blood and providing them with more ATP.

3.5.4. High-Active Animal Model

Despite the HA mice showing higher WBP and clearance capacity of VAL and ILE, the observed differences may represent other factors that affect endogenous metabolic pathways. For example, it is possible that strain differences, weight, activity exposure, or diet, could have affected VAL and ILE metabolism differentially between the strains. The basis for the difference between inbred strains is the underlying genomic variations between these strains. We have studied these two strains' genomic and proteomic profiles extensively in the past (28, 29, 43, 58, 148) to understand the underlying genomic/proteomic factors that differentially regulate the physical activity levels of these two strains. Such proteomic

differences include overexpression of succinyl-CoA ligase and a cluster of creatine kinase B in the nucleus accumbens-brain region that plays a central role in the reward circuit. Interestingly, both succinyl-CoA ligase and creatine kinase B are involved in energy metabolism. Primarily, succinyl-CoA ligase accelerates the conversion of the intermediate succinyl-CoA into succinate within the TCA cycle, and creatine kinase B plays an essential catalytic role in the transfer of phosphate between ATP and several phosphagens within tissues that have significant fluctuating energy demands (e.g., brain, skeletal muscle, heart, and liver).

Other external factors that could have influenced BCAA metabolic pathways were controlled for during this study. As a control for aging effects, both mouse groups were analyzed at 12-weeks of age (peak physically active age for most mice (149)). Additionally, while the HA group had a 6.4% higher lean mass than the LA mice, which was different from our earlier results (57), we controlled for these mass differences by standardizing our results by lean body mass. To prevent potential training-induced changes in metabolism, we studied naive animals (i.e., not exposed to a running wheel) given we have previously shown running wheel exposure can affect gene expression (33). This preventative measure reduced the potential risk of training-induced metabolic changes in our mouse stains. Lastly, as a check on potential diet-induced changes in metabolism, both strains had the same daily average food consumption, which controlled for potential differences in metabolism induced by varying caloric intake composition or volume (**Table 1**). Therefore, other than known genomic differences that have been associated with physical activity regulation, we conclude the animals studied were not exposed to other external factors that would have altered BCAA metabolism.

3.5.5. Conclusions

In conclusion, without external factors altering BCAA metabolism, differences in BCAA metabolism should be a result of alterations in various endogenous factors. As such, the decreased plasma concentrations, higher WBP, and higher clearance rates of VAL and ILE suggest that elevated oxidation of VAL and ILE to propionyl-CoA and methylmalonyl-CoA potentially increased anaplerosis through Succinyl-CoA. This increase in anaplerosis could stimulate mitochondrial energetic flux yielding more ATP production in HA mice, which may be potentially linked to their exhibition of higher PA levels.

4. ELEVATED WHOLE-BODY PRODUCTION OF PHENYLALANINE AND TYROSINE IN HIGH-ACTIVE MICE

4.1. Introduction

Moderate physical activity (PA) has been recognized to reduce the occurrence of PA-related diseases (22) such as type II diabetes, cardiovascular disease, and cancer (25); however, fewer than 10% of American adults older than 20 years of age engage in the recommended daily 30 min of moderate-intensity PA (24). To better understand the potential mechanism(s) regulating PA levels, we have studied inbred mice with innately different PA levels ─ high-active (HA) and low-active (30, 33, 43, 57, 58, 148, 149). We (38) and others have suggested (141-143) that the dopaminergic system (system associated with regulating motor movement as well as reward behavior and motivation) may be responsible for the regulation of differential PA levels. More specifically, we have shown in HA and LA mice that genetic differences in dopamine signaling may play a role in PA response to dopaminergic-acting drugs (56).

Although the dopaminergic system is complex, dopamine biosynthesis can be affected by the availability of its precursor, L-3,4-dihydroxyphenylalanine (L-DOPA) (144), which is derived from tyrosine (TYR) through hydroxylation via the enzyme tyrosine hydroxylase (TyrH) (145). TYR is a non-essential amino acid, and it is primarily synthesized in the liver from the essential amino acid phenylalanine (PHE) through PHE hydroxylase (146). While PHE and TYR metabolism plays a key precursor role in dopamine production, these two AAs also play vital metabolic roles in energy production within the tricarboxylic acid cycle (TCA). More precisely, after PHE is converted to TYR, a series of metabolic

conversion steps occur and yield acetoacetate and fumarate, which can later be converted into a ketone body and glucose, respectively, and subsequently create energy.

Moreover, the total conversion of PHE to TYR can be applied as quantification for whole-body net protein breakdown (WBnetPB) (64, 76, 77, 213). This conversion is important, as WBnetPB can provide information on total protein turnover within the muscle and whole-body tissues. Given PHE and TYR's association with the dopaminergic system, their ketogenic and glucogenic energy-producing properties, and the derived quantification of net protein breakdown, we hypothesize that TYR and PHE metabolism may be involved with the regulation of PA levels of HA and LA mice.

To determine if PHE and TYR metabolic pathways are associated with the regulation of differential PA levels in HA and LA inbred mice, we studied total AA plasma concentrations. Additionally, we used a stable tracer approach to assess whole-body production (WBP), and clearance rates of PHE and TYR, and Tau-Methyl-histidine (Tau-MetHis) ─ metabolite used as a direct measure of muscle protein breakdown which has been associated with impaired muscle weakness physical function (214).

4.2. Materials and Methods

4.2.1. Animals

All procedures were approved by the institutional animal care and use committee (IACUC) of Texas A&M University. We assessed a total of 23 male C3H/HeJ mice (inherently LA inbred strain) and 20 male C57L/J mice (inherently HA inbred strain). The characteristic activity levels of these two strains are based on previous voluntary wheel running data (57). Mice were purchased from The Jackson Laboratory (Bar Harbor, ME, USA) at 10-weeks of age and group-housed in standard mouse-cages in light and

temperature-controlled housing facility (12-hour light-dark cycle, room temperature 22-24°C). Water and a standard chow diet (Harlan Labs, Houston TX; 25.2% protein, 4.0 % fat, 39.5% carbohydrate, 3.3% crude fiber, 10% neutral fiber, and 9.9% ash) diet were provided *ad libitum.* After a two-week acclimation period, metabolic phenotyping procedures were performed via a terminal surgery. During the acclimation period, mice were not exposed to wheel-running activity for two reasons: 1) average PA levels of these two mouse strains have previously been described (57) (average wheel running distance: LA = 0.6 ± 1.1 km/day; HA = 9.5 ± 2.0 km/day); and 2) we have shown that multiple day exposure to running wheels can induce physiological changes due to exercise adaptation (33).

4.2.2. Study Protocol

Four hours before commencement of surgical procedures, food was removed from mouse cages to study animals in a post-absorptive condition. Body composition was assessed post food removal, and mice were then placed in clean cages and left undisturbed until the start of surgical procedure (**Figure 1**). All metabolic testing was performed using a terminal surgical procedure adapted from Hallemeesch et al. (160), which consisted of sedating the animal and a jugular vein catheterization for delivery of isotope tracer bolus and sample collection (**Figure 1**). The study protocol was identical for both groups and lasted approximately 5.5 hours.

4.2.3. Body Composition

Bodyweight (bw) was assessed immediately after food withdrawal using a digital beam scale with lean body mass, fat mass, percent fat mass, total water, and free water measured via echo MRI (EchoMRI LLC, Houston, TX 77079; **Table 1**). Bone mineral

density data were collected by dual-energy X-ray absorptiometry (DEXA [Lunar PIXImus densitometer, GE Lunar Corp. Fitchburg, WI]) while the animals were under anesthesia.

4.2.4. Anesthesia Induction

Mice were anesthetized via intraperitoneal (IP) injection (0.1 ml/10g body weight) containing a mixture of ketamine (1.25 mg/10g BW) and medetomidine (2 μg/10g BW) (160). Anesthesia was maintained using a continuous pump infusion of ketamine (0.35 mg/ 10 g bw/h) and medetomidine (0.35 μg/10g bw/h) at a rate of 0.1 ml/10 g bw/h, given subcutaneously (160). Fluid balance and blood pressure were maintained by an initial 1.5 ml IP saline injection (0.9% sterile, NaCl), and by continuous pump infusion (Harvard PHD2000) of saline at a rate of 2.5 ml/hour delivered subcutaneously (160). Breathing was continuously monitored, and body temperature was monitored using a rectal thermistor and maintained at 37°C via *a heating* pad and lamp.

4.2.5. Stable Tracer Infusion by IV Pulse

Under anesthesia, a peripheral catheter was placed in the right jugular vein for blood sampling and infusion of a stable isotope tracer pulse (0.1 ml; isotonic) containing L-(Ring-$^{13}C_6$)-PHE, L-(Ring-D_4)-TYR, and L-(Methyl-D_3)-Tau-MetHis (Cambridge Isotope Laboratories: Woburn, MA, USA). The different concentrations (nmol/0.01 ml) for each tracer are as follows: PHE (271.8), TYR (161.1), and Tau-MetHis (38.2). Blood samples (0.05- 0.1 ml per sample) were collected utilizing two sampling time schedules (schedule 1: t = 1, 5, 10, 20, and 30 minutes; schedule 2: t = 3, 7, 15, 25, and 40 minutes) after pulse administration (Figure 1).

Mice were sampled according to schedule 1 or 2 in order to minimize the total volume of blood taken from each animal and to provide a wider range of temporal points for

more accurate fitting of the resulting data. The volume of blood that was collected was replaced with an equal volume of sterile normal saline. In a preliminary study in which no tracer infusion occurred during the mouse surgery, we obtained blood samples to measure the background enrichment. After the cannulation and sampling procedure concluded, the animals were euthanized by removal of the heart. Venous lithium-heparinized blood was collected and immediately placed on ice. Within one hour, the blood samples were centrifuged (4 °C, 3120 x *g* for 5 min) to obtain plasma, which was then deproteinized with 0.1 vol of 33% (w/w) trichloroacetic acid and stored at −80 °C for later analysis of tracer enrichments and concentrations of AAs via liquid chromatography tandem-mass spectrometry (LC-MS/MS).

4.2.6. Biochemical Analysis

Plasma AAs and their tracer enrichments were measured batchwise with LC-MS/MS using procedures previously validated in our lab (49, 161-163). Isotope peak areas were automatically identified and integrated by the SignalFinder1 algorithm in MultiQuant v. 3.0 (Sciex), exported to Excel for calculation of area ratios, and regressed using GraphPad Prism 8 as described in detail in our previous study (49)

4.2.7. Calculations

The decay (change over time) of the tracer/tracee ratio (TTR [injected stable tracers/naturally occurring AA being traced]) was group fitted with a two-exponential least-squares regression: $TTR(t) = a*\exp(-k1*t) + b*\exp(-k2*t)$. The area under the curve (AUC) was calculated from the integral two exponential curves (76). Whole-body production (WBP) was then calculated as DOSE (amount of isotope tracer in the

pulse)/AUC. Metabolites from the injected stable tracers were group fitted as TTR (t) = −a*exp(−k1*t) + b*exp(−k2*t), and the integral was calculated to represent the AUC.

We calculated the conversion of one AA into another AA by using the WBP of the product AA and the ratio between the AUC of the TTR from the pulse of the product/substrate (49). For example, we defined net protein breakdown by calculating the conversion of PHE to TYR as the Ra TYR (L-[$^{13}C_9$-15N]-TYR) * TTR(L-[ring-$^{2}H_4$]-TYR)/TTR (L-[ring-$^{2}H_5$]-PHE). The non-compartmental analysis was done using GraphPad Prism (version 8.1). Additionally, the clearance flux of the stable tracers was calculated as WBP/plasma concentration (67) and expressed as mL/min.

4.2.8. Statistical Analysis

Results are expressed as mean ± standard error (SE). If data failed normality or equal variance tests, they were log-transformed. Unpaired Student's *t*-tests were used to determine differences in body composition, plasma AA, and plasma metabolites between the HA and LA mouse groups. The statistical package within GraphPad Prism (Version 8.1) was used for data analysis. The level of significance was set *a priori* at $p < 0.05$.

4.3. Results

A total of 23 LA and 20 HA male mice were analyzed at twelve-weeks of age (**Table 1**). Although no differences in total fat mass, bone mineral density, or average daily food consumption were observed, the HA mice were characterized by 6.7% higher total body weight ($p<0.0001$) due to a 6.4% higher lean mass ($p=0.0003$). The higher lean mass observed in the HA mice also explains the 7.0% higher total-body water observed in these mice. It should be noted that although the lean mass was higher in the HA mice, it only represents a 1.4 g difference in lean mass between HA and LA mice, thus suggesting that

any differences observed in WBP and clearance rates could be associated with the difference in lean body mass. For this reason, we normalized our results to the animal's lean body mass. The same statement can be applied to the total body water differences as they account for a 1.3 g difference between mouse strains.

Post-absorptive plasma concentrations of the measured AAs are depicted in **Table 1**. Significantly lower plasma concentrations were observed in the HA mice for TYR (26.6%, $p < 0.0001$), while Tau-MetHis concentrations were significantly higher (15.0%, $p = 0.0011$) in HA mice. Although plasma concentrations for PHE were 11% lower in HA mice, the observed difference was not significantly different ($p=0.0724$). Despite lower TYR and higher Tau-MetHis plasma concentrations in the HA mice, we found HA mice had significantly higher WBP for TYR (10.18%, $p < 0.05$; **Figure 9**), while having no significant difference in WBP of Tau-MetHis ($p = 0.1516$; **Figure 10**). Additionally, despite no differences in the plasma concentrations of PHE, the HA mice had significantly higher WBP of PHE (7.6%, $p < 0.01$; **Figure- 11**). Additionally, we found no differences in the conversion of PHE to TYR (i.e., net protein breakdown) ($p = 0.28$). The HA group had an 18.5% increased clearance rate for PHE, 36.5% for TYR, and 22.0% for Tau-MetHis (all p values < 0.0001) compared to the LA group (**Figure 12**).

4.4. Discussion

Our purpose was to determine if PHE and TYR metabolic pathways were associated with different physical activity levels. Overall, our data suggest HA mice have elevated PHE and TYR related pathways that may be associated with their high PA levels. The modification of these pathways includes plasma concentrations, whole-body production, and clearance. The observed differences in VAL and ILE could lead to increases in dopamine

production and/or improved anaplerosis in HA mice, which may be associated with their inherently high PA levels.

4.4.1. Dopamine Production and Physical Activity

Dopamine was first associated with basic motor function during a study by Bernheimer et al. (215) in which Parkinson's syndrome characterized sporadic and uncontrollable movements due to decreased dopamine concentrations within the brain striatum and pallidum of patients with the syndrome (215). A later study suggested that dopamine deficiency was associated with severe PA reduction (142) by blunting the dopaminergic reward system. While additional studies suggested similar associations (38, 42, 56, 216, 217), it is difficult to pinpoint the exact mechanism within the dopaminergic neurological cascade that may be responsible for decreased PA levels in the previous studies.

Here, we speculate that increased WBP (**Figures 9 and 11**) and clearance rates (**Figure 12**) of PHE and TYR may be responsible for increasing dopamine, and subsequently associated with the high PA levels in HA mice. Although speculative, given that dopamine nor its precursor L-DOPA (144) were assessed, the logic that more TYR contributes to more dopamine parallels with our current results and previous dopaminergic studies in HA and LA mice (38, 42, 56).

4.4.2. Can PHE and TYR Stimulate Anaplerosis?

While PHE and TYR metabolism plays a key precursor role in dopamine production, PHE and TYR are two of four AA considered to serve as both ketogenic and glucogenic substrates in energy production, with the other two AA being ILE and tryptophan (138). Like the VAL and ILE anaplerosis discussion in section three, liver cells can metabolize PHE and TYR ultimately forming acetyl acetate and fumarate (139). Acetyl acetate can then be

converted into ketone bodies while fumarate can form glucose (**Figure 13**). However, this PHE and TYR conversion to fuel molecules can only occur after PHE is converted to TYR by the enzyme phenylalanine dehydrogenase, followed by several additional conversion steps (a-hydroxyphenylpyruvate → homogentisate → 4-maleylacetoacetate → 4-fumerylacetoacetate), thus yielding fumarate and acetyl acetate (139, 218).

Subsequently, fumarate is converted to malate then into oxaloacetate ─ the starting point for gluconeogenesis in the liver - while TYR derived acetyl acetate forms acetoacetyl-CoA via 3-ketoacyl-CoA transferase and then produces a ketone body. Thus. PHE and TYR can stimulate anaplerosis. The observed elevation of PHE and TYR in HA mice suggests that HA mice may have a greater capacity to generate fuel molecules via anaplerosis than LA mice.

4.4.3. Whole-Body Net Protein Breakdown and Tau-Methylhistidine

WBnetPB can be quantified by calculating the total conversion of PHE to TYR (64, 76, 77, 213). Tau-MetHis is present in actin and myosin heavy-chain proteins and is a commonly used biomarker to determine myofibrillar protein breakdown (MPB) (73, 219-221). In our study, both WBnetPB and tau-MetHis are important measurements because elevations in WBnetPB in combination with elevated tau-MetHis have been associated with muscle weakness and decreased physical function (50, 76, 214, 222-224). Interestingly, the lack of observed differences in WBnetPB and tau-MetHis (**Figure 10**) suggest that PHE and TYR turnover within the muscle tissue is constant and thus the elevated PHE and TYR we observed are derived from different tissues such as the liver and/or brain.

4.4.4. Conclusion

The decreased plasma concentrations, higher WBP, and higher clearance rates of PHE and TYR suggest that elevation in these AA could lead to increases in dopamine production *via* increased L-DOPA synthesis. Additionally, PHE and TYR's ketogenic and glucogenic properties suggest an increase in energy production *via* increased anaplerosis. As such, both the dopaminergic and anaplerotic metabolic pathways could be associated with the inherently high PA levels observed in HA mice. Moreover, the lack of differences in tau-MetHis and WBnetPB suggest that muscle-derived PHE is constant, and thus, the observed elevated PHE and TYR in HA mice is likely derived from other body tissue(s).

5. CONCLUSIONS

Our untargeted amino acid metabolism results add insight into metabolic pathways potentially associated with different physical activity levels. This stable isotope tracer phenotyping study suggested three different amino acid metabolic pathways, which may be associated with differential physical activity levels in HA and LA mice. However, since this was an untargeted study, results depicted in sections 2-4 are associative, and as such, hypothesis-driven studies should be considered for follow-up investigations.

Section two suggested the high physical activity levels characteristic to HA mice were associated with an activated ARG pathway. Moreover, the higher ratio of NO production in HA mice suggested the activated ARG pathway may serve as a precursor to increasing NO production, which may be potentially linked to their exhibition of higher physical activity levels. However, despite utilizing established prediction equations (49, 172) to quantify NO production, NO was not directly measured in this study. Thus, future studies NO levels should be measured directly to test the hypothesis that NO is involved in determining differential physical activity levels.

Section three provided insight into the BCAA ─ VAL, ILE, and LEU. Our data suggested that VAL and ILE differences in plasma concentrations, WBP, and clearance rates were due to elevated VAL and ILE oxidation to propionyl-CoA and methylmalonyl-CoA. As a result, we speculated that the increased oxidation raised anaplerosis through the TCA cycle intermediate succinyl-CoA and subsequently stimulated mitochondrial energetic flux. This stimulation of mitochondrial energetic flux could yield more ATP production in HA mice, which could be linked to their exhibition of higher PA levels.

In section four, our data showed that HA mice had elevated WBP and clearance of PHE and TYR, which explain the lower plasma concentrations for the same AA. These results were similar to the VAL and ILE kinetics observed in section three. We would speculate that the observed differences in PHE and TYR could lead to increases in dopamine production *via* increased L-DOPA synthesis. Additionally, PHE and TYR's ketogenic and glucogenic properties provide a basis for the suggestion that an increase in energy production could occur *via* increased anaplerosis. As such, both the dopaminergic and anaplerotic metabolic pathways may be associated with the inherently high PA levels observed in HA mice. Moreover, the lack of differences in tau-MethHis and PHE to TYR WBnetPB, suggest that muscle-derived PHE is constant; thus, the observed elevated PHE and TYR in HA mice is likely derived from other body tissue(s).

In conclusion, the proposed ARG-NO, BCAA, and PHE-TYR metabolic pathways may employ potential regulatory roles in different PA levels. However, due to the untargeted exploratory nature of this study, our suggested pathways are associative and speculative. Studies directly targeting these proposed metabolic pathways should consider analyzing NO, keto-acid intermediates derived from BCAA breakdown, and dopamine, including dopaminergic receptors and precursors. Additionally, tissue-specific (e.g., muscle, brain, liver, heart, adipose, small intestine, and kidney) amino acid kinetics – currently planned for the tissues from this study - will provide a more comprehensive metabolic picture of the differential pathways existing between animals exhibiting inherent high and low-activity pattern.

REFERENCES

1. Lamonte MJ. Physical activity and diabetes prevention. 2005;99(3):1205-13. doi: 10.1152/japplphysiol.00193.2005.

2. Hamman RF, Wing RR, Edelstein SL, et al. Effect of Weight Loss With Lifestyle Intervention on Risk of Diabetes. Diabetes Care. 2006;29(9):2102-7. doi: 10.2337/dc06-0560.

3. Reduction in the Incidence of Type 2 Diabetes with Lifestyle Intervention or Metformin. New England Journal of Medicine. 2002;346(6):393-403. doi: 10.1056/nejmoa012512.

4. Tuomilehto J, Lindström J, Eriksson JG, et al. Prevention of Type 2 Diabetes Mellitus by Changes in Lifestyle among Subjects with Impaired Glucose Tolerance. New England Journal of Medicine. 2001;344(18):1343-50. doi: 10.1056/nejm200105033441801.

5. Manson JE, Hu FB, Rich-Edwards JW, et al. A Prospective Study of Walking as Compared with Vigorous Exercise in the Prevention of Coronary Heart Disease in Women. 1999;341(9):650-8. doi: 10.1056/nejm199908263410904.

6. Kokkinos P, Myers J, Faselis C, et al. Exercise Capacity and Mortality in Older Men: A 20-Year Follow-Up Study. 2010;122(8):790-7. doi: 10.1161/circulationaha.110.938852.

7. Joyner MJ, Green DJ. Exercise protects the cardiovascular system: effects beyond traditional risk factors. The Journal of physiology. 2009;587(23):5551-8. doi: 10.1113/jphysiol.2009.179432.

8. Weinstein AR, Sesso HD. Joint effects of physical activity and body weight on diabetes and cardiovascular disease. Exerc Sport Sci Rev. 2006;34(1):10-5. Epub 2006/01/06. PubMed PMID: 16394809.

9. Campbell KL, McTiernan A. Exercise and Biomarkers for Cancer Prevention Studies. The Journal of nutrition. 2007;137(1):161S-9S. doi: 10.1093/jn/137.1.161s.

10. Colditz GA, Cannuscio CC, Frazier AL. Physical activity and reduced risk of colon cancer: implications for prevention. Cancer Causes Control. 1997;8(4):649-67. Epub 1997/07/01. PubMed PMID: 9242482.

11. Moore SC, Gierach GL, Schatzkin A, Matthews CE. Physical activity, sedentary behaviours, and the prevention of endometrial cancer. 2010;103(7):933-8. doi: 10.1038/sj.bjc.6605902.

12. Monninkhof EM, Elias SG, Vlems FA, et al. Physical Activity and Breast Cancer. Epidemiology. 2007;18(1):137-57. doi: 10.1097/01.ede.0000251167.75581.98.

13. Wolff I, Van Croonenborg JJ, Kemper HCG, Kostense PJ, Twisk JWR. The Effect of Exercise Training Programs on Bone Mass: A Meta-analysis of Published Controlled Trials in Pre- and Postmenopausal Women. Osteoporosis International. 1999;9(1):1-12. doi: 10.1007/s001980050109.

14. Yaffe K, Barnes D, Nevitt M, Lui L-Y, Covinsky K. A Prospective Study of Physical Activity and Cognitive Decline in Elderly Women. Archives of Internal Medicine. 2001;161(14):1703. doi: 10.1001/archinte.161.14.1703.

15. Slentz CA, Duscha BD, Johnson JL, et al. Effects of the Amount of Exercise on Body Weight, Body Composition, and Measures of Central Obesity. Archives of Internal Medicine. 2004;164(1):31. doi: 10.1001/archinte.164.1.31.

16. Kramer AF, Colcombe S. Fitness Effects on the Cognitive Function of Older Adults: A Meta-Analytic Study—Revisited. Perspectives on Psychological Science. 2018;13(2):213-7. doi: 10.1177/1745691617707316.

17. Lee IM. Physical Activity and Weight Gain Prevention. JAMA. 2010;303(12):1173. doi: 10.1001/jama.2010.312.

18. Dik MG, Deeg DJH, Visser M, Jonker C. Early Life Physical Activity and Cognition at Old Age. Journal of Clinical and Experimental Neuropsychology. 2003;25(5):643-53. doi: 10.1076/jcen.25.5.643.14583.

19. Booth FW, Roberts CK, Laye MJ. Lack of exercise is a major cause of chronic diseases. Compr Physiol. 2012;2(2):1143-211. Epub 2012/04/01. doi: 10.1002/cphy.c110025. PubMed PMID: 23798298; PubMed Central PMCID: PMCPMC4241367.

20. Mokdad AH, Marks JS, Stroup DF, Gerberding JL. Correction: actual causes of death in the United States, 2000. JAMA. 2005;293(3):293-4. Epub 2005/01/20. doi: 10.1001/jama.293.3.293. PubMed PMID: 15657315.

21. Ding D, Lawson KD, Kolbe-Alexander TL, et al. The economic burden of physical inactivity: a global analysis of major non-communicable diseases. The Lancet. 2016;388(10051):1311-24. doi: 10.1016/s0140-6736(16)30383-x.

22. Kelly P, Kahlmeier S, Götschi T, et al. Systematic review and meta-analysis of reduction in all-cause mortality from walking and cycling and shape of dose response relationship. International Journal of Behavioral Nutrition and Physical Activity. 2014;11(1). doi: 10.1186/s12966-014-0132-x.

23. Levine JA, McCrady SK, Lanningham-Foster LM, Kane PH, Foster RC, Manohar CU. The Role of Free-Living Daily Walking in Human Weight Gain and Obesity. 2008;57(3):548-54. doi: 10.2337/db07-0815.

24. Troiano RP, Berrigan D, Dodd KW, Mâsse LC, Tilert T, McDowell M. Physical Activity in the United States Measured by Accelerometer. 2008;40(1):181-8. doi: 10.1249/mss.0b013e31815a51b3.

25. Booth FW, Roberts CK, Thyfault JP, Ruegsegger GN, Toedebusch RG. Role of Inactivity in Chronic Diseases: Evolutionary Insight and Pathophysiological Mechanisms. Physiological Reviews. 2017;97(4):1351-402. doi: 10.1152/physrev.00019.2016. PubMed PMID: 28814614.

26. Letsinger AC, Granados JZ, Little SE, Lightfoot JT. Alleles associated with physical activity levels are estimated to be older than anatomically modern humans. PloS one. 2019;14(4):e0216155. doi: 10.1371/journal.pone.0216155.

27. Schmitt EE, Vellers HL, Porter WW, Lightfoot JT. Environmental Endocrine Disruptor Affects Voluntary Physical Activity in Mice. Medicine and science in sports and exercise. 2016;48(7):1251-8. Epub 2016/02/20. doi: 10.1249/mss.0000000000000908. PubMed PMID: 26895396; PubMed Central PMCID: PMCPMC4911329.

28. Ferguson DP, Dangott LJ, Vellers HL, Schmitt EE, Lightfoot JT. Differential protein expression in the nucleus accumbens of high and low active mice. Behavioural brain research. 2015;291:283-8. Epub 2015/05/27. doi: 10.1016/j.bbr.2015.05.035. PubMed PMID: 26008157.

29. Dawes M, Kochan KJ, Riggs PK, Timothy Lightfoot J. Differential miRNA expression in inherently high- and low-active inbred mice. Physiological reports. 2015;3(7). doi: 10.14814/phy2.12469.

30. Ferguson DP, Dangott LJ, Schmitt EE, Vellers HL, Lightfoot JT. Differential skeletal muscle proteome of high- and low-active mice. Journal of applied physiology (Bethesda, Md : 1985). 2014;116(8):1057-67. Epub 2014/02/08. doi: 10.1152/japplphysiol.00911.2013. PubMed PMID: 24505100; PubMed Central PMCID: PMCPMC4035790.

31. Ferguson DP, Dangott LJ, Lightfoot JT. Lessons learned from vivo-morpholinos: How to avoid vivo-morpholino toxicity. Biotechniques. 2014;56(5):251-6. Epub 2014/05/09. doi: 10.2144/000114167. PubMed PMID: 24806225; PubMed Central PMCID: PMCPMC4182913.

32. de Geus EJ, Bartels M, Kaprio J, Lightfoot JT, Thomis M. Genetics of regular exercise and sedentary behaviors. Twin research and human genetics : the official journal of the International Society for Twin Studies. 2014;17(4):262-71. Epub 2014/07/19. doi: 10.1017/thg.2014.42. PubMed PMID: 25034445.

33. Dawes M, Moore-Harrison T, Hamilton AT, et al. Differential gene expression in high- and low-active inbred mice. BioMed research international. 2014;2014:361048. Epub 2014/02/20. doi: 10.1155/2014/361048. PubMed PMID: 24551844; PubMed Central PMCID: PMCPMC3914289.

34. Lightfoot JT. Why control activity? Evolutionary selection pressures affecting the development of physical activity genetic and biological regulation. BioMed research international. 2013;2013:821678. Epub 2014/01/24. doi: 10.1155/2013/821678. PubMed PMID: 24455728; PubMed Central PMCID: PMCPMC3884604.

35. Bowen RS, Knab AM, Hamilton AT, McCall JR, Moore-Harrison TL, Lightfoot JT. Effects of Supraphysiological Doses of Sex Steroids on Wheel Running Activity in Mice. Journal of steroids & hormonal science. 2012;3(2):110. Epub 2012/11/01. doi: 10.4172/2157-7536.1000110. PubMed PMID: 25419484; PubMed Central PMCID: PMCPMC4236312.

36. Bowen RS, Turner MJ, Lightfoot JT. Sex hormone effects on physical activity levels: why doesn't Jane run as much as Dick? Sports medicine (Auckland, NZ). 2011;41(1):73-86. Epub 2010/12/15. doi: 10.2165/11536860-000000000-00000. PubMed PMID: 21142285; PubMed Central PMCID: PMCPMC3050489.

37. Bowen RS, Ferguson DP, Lightfoot JT. Effects of Aromatase Inhibition on the Physical Activity Levels of Male Mice. Journal of steroids & hormonal science. 2011;1(1):1-7. Epub 2011/11/25. doi: 10.4172/2157-7536.s1-001. PubMed PMID: 23483029; PubMed Central PMCID: PMCPMC3593090.

38. Knab AM, Lightfoot JT. Does the difference between physically active and couch potato lie in the dopamine system? International journal of biological sciences. 2010;6(2):133-50. Epub 2010/03/13. PubMed PMID: 20224735; PubMed Central PMCID: PMCPMC2836544.

39. Leamy LJ, Pomp D, Lightfoot JT. Genetic variation in the pleiotropic association between physical activity and body weight in mice. Genet Sel Evol. 2009;41:41. Epub 2009/09/25. doi: 10.1186/1297-9686-41-41. PubMed PMID: 19775457; PubMed Central PMCID: PMCPMC2760520.

40. Leamy LJ, Pomp D, Lightfoot JT. Genetic variation for body weight change in mice in response to physical exercise. BMC genetics. 2009;10:58. Epub 2009/09/24. doi: 10.1186/1471-2156-10-58. PubMed PMID: 19772584; PubMed Central PMCID: PMCPMC2760581.

41. Knab AM, Bowen RS, Moore-Harrison T, Hamilton AT, Turner MJ, Lightfoot JT. Repeatability of exercise behaviors in mice. Physiology & behavior. 2009;98(4):433-40. Epub 2009/07/22. doi: 10.1016/j.physbeh.2009.07.006. PubMed PMID: 19619567; PubMed Central PMCID: PMCPMC2746869.

42. Knab AM, Bowen RS, Hamilton AT, Gulledge AA, Lightfoot JT. Altered dopaminergic profiles: implications for the regulation of voluntary physical activity. Behavioural brain research. 2009;204(1):147-52. Epub 2009/06/13. doi: 10.1016/j.bbr.2009.05.034. PubMed PMID: 19520120; PubMed Central PMCID: PMCPMC2723172.

43. Lightfoot JT, Turner MJ, Pomp D, Kleeberger SR, Leamy LJ. Quantitative trait loci for physical activity traits in mice. Physiological genomics. 2008;32(3):401-8. Epub 2008/01/04. doi: 10.1152/physiolgenomics.00241.2007. PubMed PMID: 18171721; PubMed Central PMCID: PMCPMC2745307.

44. Vellers HL, Letsinger AC, Walker NR, Granados JZ, Lightfoot JT. High Fat High Sugar Diet Reduces Voluntary Wheel Running in Mice Independent of Sex Hormone Involvement. Frontiers in physiology. 2017;8(628). doi: 10.3389/fphys.2017.00628.

45. Meek TH, Eisenmann JC, Garland T, Jr. Western diet increases wheel running in mice selectively bred for high voluntary wheel running. International journal of obesity (2005). 2010;34(6):960-9. Epub 2010/02/17. doi: 10.1038/ijo.2010.25. PubMed PMID: 20157317.

46. Luiking YC, Poeze M, Deutz NE. A randomized-controlled trial of arginine infusion in severe sepsis on microcirculation and metabolism. Clinical Nutrition. 2019. doi: 10.1016/j.clnu.2019.08.013.

47. Engelen MPKJ, Ten Have GAM, Thaden JJ, Deutz NEP. New advances in stable tracer methods to assess whole-body protein and amino acid metabolism. Current opinion in clinical nutrition and metabolic care. 2019;22(5):337-46. doi: 10.1097/mco.0000000000000583.

48. Ten Have GAM, Deutz RCI, Engelen M, Wolfe RR, Deutz NEP. Characteristics of a Pseudomonas aeruginosa induced porcine sepsis model for multi-organ metabolic flux measurements. Lab Anim. 2018;52(2):163-75. Epub 2017/07/07. doi: 10.1177/0023677217718003. PubMed PMID: 28679339.

49. Deutz NEP, Thaden JJ, ten Have GAM, Walker DK, Engelen MPKJ. Metabolic phenotyping using kinetic measurements in young and older healthy adults. Metabolism. 2018;78:167-78. doi: https://doi.org/10.1016/j.metabol.2017.09.015.

50. Ten Have GAM, Engelen M, Wolfe RR, Deutz NEP. Phenylalanine isotope pulse method to measure effect of sepsis on protein breakdown and membrane transport in the pig. American journal of physiology Endocrinology and metabolism. 2017;312(6):E519-E29. Epub 2017/03/16. doi: 10.1152/ajpendo.00351.2016. PubMed PMID: 28292760; PubMed Central PMCID: PMCPMC5494580.

51. Ten Have GA, Engelen MP, Wolfe RR, Deutz NE. Increased muscle myofibrillar protein breakdown rates using 3-methyl-histidine (tau-mHIS) stable isotopes in a Pseudomonas aeroginosa (PM) induced hyperdynamic sepsis pig model. The FASEB Journal. 2016;30(1 Supplement):lb761-lb.

52. de Betue CT, Deutz NE. Changes in arginine metabolism during sepsis and critical illness in children. Nestle Nutr Inst Workshop Ser. 2013;77:17-28. Epub 2013/10/11. doi: 10.1159/000351370. PubMed PMID: 24107493.

53. Ten Have GA, Engelen MP, Wolfe RR, Deutz NE. Muscle breakdown determines Arginine (ARG) availability during hyperdynamic sepsis in the pig. The FASEB Journal. 2012;26(1_MeetingAbstracts):43.7.

54. Luiking YC, Ten Have GA, Wolfe RR, Deutz NE. Arginine de novo and nitric oxide production in disease states. American journal of physiology Endocrinology and metabolism. 2012;303(10):E1177-89. Epub 2012/09/27. doi: 10.1152/ajpendo.00284.2012. PubMed PMID: 23011059; PubMed Central PMCID: PMCPMC3517635.

55. Ten Have GAM, Jalan R, Deutz NEP. Decreased circulating arginine in ALF mice does not compromise whole body NO production. Eur J Gastroen Hepat. 2007;19(10):A16-A. PubMed PMID: WOS:000254356500059.

56. Knab AM, Bowen RS, Hamilton AT, Lightfoot JT. Pharmacological manipulation of the dopaminergic system affects wheel-running activity in differentially active mice. J Biol Regul Homeost Agents. 2012;26(1):119-29. PubMed PMID: 22475103.

57. Lightfoot JT, Leamy L, Pomp D, et al. Strain screen and haplotype association mapping of wheel running in inbred mouse strains. Journal of applied physiology (Bethesda, Md : 1985). 2010;109(3):623-34. Epub 2010/06/12. doi: 10.1152/japplphysiol.00525.2010. PubMed PMID: 20538847; PubMed Central PMCID: PMCPMC2944645.

58. Leamy LJ, Pomp D, Lightfoot JT. A search for quantitative trait loci controlling within-individual variation of physical activity traits in mice. BMC genetics. 2010;11:83. Epub 2010/09/23. doi: 10.1186/1471-2156-11-83. PubMed PMID: 20858254; PubMed Central PMCID: PMCPMC2949740.

59. Jung AP, Curtis TS, Turner MJ, Lightfoot JT. Physical Activity and Food Consumption in High- and Low-Active Inbred Mouse Strains. 2010;42(10):1826-33. doi: 10.1249/mss.0b013e3181daf5e8.

60. Lightfoot JT, EJC DEG, Booth FW, et al. Biological/Genetic Regulation of Physical Activity Level: Consensus from GenBioPAC. Medicine and science in sports and exercise. 2018;50(4):863-73. Epub 2017/11/23. doi: 10.1249/mss.0000000000001499. PubMed PMID: 29166322.

61. Edfors F, Danielsson F, Hallström BM, et al. Gene-specific correlation of RNA and protein levels in human cells and tissues. Molecular Systems Biology. 2016;12(10):883. doi: 10.15252/msb.20167144.

62. Maier T, Güell M, Serrano L. Correlation of mRNA and protein in complex biological samples. FEBS Letters. 2009;583(24):3966-73. doi: 10.1016/j.febslet.2009.10.036.

63. Gry M, Rimini R, Strömberg S, et al. Correlations between RNA and protein expression profiles in 23 human cell lines. 2009;10(1):365. doi: 10.1186/1471-2164-10-365.

64. Ten Have GA, Engelen MP, Wolfe RR, Deutz NE. Using the phenylalanine (PHE) stable isotope pulse method to measure intracellular protein breakdown and metabolic shunting in the context of sepsis in the pig. The FASEB Journal. 2012;26(1_MeetingAbstracts):42.1.

65. Wilkinson DJ. Historical and contemporary stable isotope tracer approaches to studying mammalian protein metabolism. Mass Spectrom Rev. 2018;37(1):57-80. Epub 2016/05/18. doi: 10.1002/mas.21507. PubMed PMID: 27182900; PubMed Central PMCID: PMCPMC5763415.

66. Kim IY, Suh SH, Lee IK, Wolfe RR. Applications of stable, nonradioactive isotope tracers in in vivo human metabolic research. Exp Mol Med. 2016;48:e203. Epub 2016/01/23. doi: 10.1038/emm.2015.97. PubMed PMID: 26795236; PubMed Central PMCID: PMCPMC4686699.

67. Wolfe RR. Isotope Tracers in Metabolic research. 2nd, editor. New Jersey: John Wiley & Sons, Inc.; 2005. 24-6 p.

68. Walker DK, Thaden JJ, Wierzchowska-McNew A, Engelen M, Deutz NEP. Determination of beta-hydroxy-beta-methylbutyrate concentration and enrichment in human plasma using chemical ionization gas chromatography tandem mass spectrometry. Journal of chromatography B, Analytical technologies in the biomedical and life sciences. 2017;1040:233-8. Epub 2016/11/20. doi: 10.1016/j.jchromb.2016.11.010. PubMed PMID: 27856194; PubMed Central PMCID: PMCPMC5191936.

69. de Blaauw I, Heeneman S, Deutz NE, von Meyenfeldt MF. Increased whole-body protein and glutamine turnover in advanced cancer is not matched by an increased muscle protein and glutamine turnover. The Journal of surgical research. 1997;68(1):44-55. Epub 1997/02/15. doi: 10.1006/jsre.1997.5007. PubMed PMID: 9126194.

70. Engelen MP, Com G, Wolfe RR, Deutz NE. Dietary essential amino acids are highly anabolic in pediatric patients with cystic fibrosis. J Cyst Fibros. 2013;12(5):445-53. Epub 2013/01/30. doi: 10.1016/j.jcf.2012.12.011. PubMed PMID: 23357545; PubMed Central PMCID: PMCPMC3640686.

71. Fouillet H, Gaudichon C, Mariotti F, et al. Compartmental modeling of postprandial dietary nitrogen distribution in humans. American journal of physiology Endocrinology and metabolism. 2000;279(1):E161-75. Epub 2000/07/14. doi: 10.1152/ajpendo.2000.279.1.E161. PubMed PMID: 10893336.

72. Rakotoambinina B. Taurine kinetics assessed using [1,2-13C2]taurine in healthy adult humans. 2004;287(2):E255-E62. doi: 10.1152/ajpendo.00333.2003.

73. Rathmacher JA, Nissen SL. Development and application of a compartmental model of 3-methylhistidine metabolism in humans and domestic animals. Advances in experimental medicine and biology. 1998;445:303-24. Epub 1998/10/22. doi: 10.1007/978-1-4899-1959-5_20. PubMed PMID: 9781398.

74. Wu F, Yang F, Vinnakota KC, Beard DA. Computer Modeling of Mitochondrial Tricarboxylic Acid Cycle, Oxidative Phosphorylation, Metabolite Transport, and Electrophysiology. 2007;282(34):24525-37. doi: 10.1074/jbc.m701024200.

75. Beard DA, Liang S-D, Qian H. Energy Balance for Analysis of Complex Metabolic Networks. 2002;83(1):79-86. doi: 10.1016/s0006-3495(02)75150-3.

76. Mason A, Engelen M, Ivanov I, Toffolo GM, Deutz NEP. A four-compartment compartmental model to assess net whole body protein breakdown using a pulse of phenylalanine and tyrosine stable isotopes in humans. American journal of physiology Endocrinology and metabolism. 2017;313(1):E63-E74. Epub 2017/03/09. doi: 10.1152/ajpendo.00362.2016. PubMed PMID: 28270442; PubMed Central PMCID: PMCPMC6109702.

77. Mason A, Engelen M, Toffolo G, Deutz N. A Comprehensive Compartmental Model for the Assessment of Net Whole Body Protein Breakdown, Using a Pulse of Phenylalanine and Tyrosine Stable Isotopes in Humans. The FASEB Journal. 2016;30(1 Supplement):lb391-lb.

78. Mariotti F, Petzke KJ, Bonnet D, et al. Kinetics of the utilization of dietary arginine for nitric oxide and urea synthesis: insight into the arginine-nitric oxide metabolic system in humans. Am J Clin Nutr. 2013;97(5):972-9. Epub 2013/03/29. doi: 10.3945/ajcn.112.048025. PubMed PMID: 23535108.

79. Bregendahl K, Yang X, Liu L, et al. Fractional protein synthesis rates are similar when measured by intraperitoneal or intravenous flooding doses of L-[ring-2H5]phenylalanine in combination with a rapid regimen of sampling in piglets. The Journal of nutrition. 2008;138(10):1976-81. Epub 2008/09/23. doi: 10.1093/jn/138.10.1976. PubMed PMID: 18806110.

80. Zhang XJ, Chinkes DL, Herndon DN, Wolfe RR. Measurement of protein fractional synthesis and breakdown rates in the skin of rabbits using a subflooding dose method. Metabolism. 2009;58(9):1239-47. Epub 2009/06/06. doi: 10.1016/j.metabol.2009.03.022. PubMed PMID: 19497598.

81. Zhang X-J, Chinkes DL, Wolfe RR. Measurement of muscle protein fractional synthesis and breakdown rates from a pulse tracer injection. 2002;283(4):E753-E64. doi: 10.1152/ajpendo.00053.2002.

82. McCarthy O, Moser O, Eckstein ML, Bain SC, Pitt J, Bracken R. Supplementary Nitric Oxide Donors and Exercise as Potential Means to Improve Vascular Health in People with Type 1 Diabetes: Yes to NO? Nutrients. 2019;11(7). Epub 2019/07/25. doi: 10.3390/nu11071571. PubMed PMID: 31336832; PubMed Central PMCID: PMCPMC6682901.

83. Tsukiyama Y, Ito T, Nagaoka K, Eguchi E, Ogino K. Effects of exercise training on nitric oxide, blood pressure and antioxidant enzymes. Journal of Clinical Biochemistry and Nutrition. 2017;60(3):180-6. doi: 10.3164/jcbn.16-108. PubMed PMID: WOS:000403033800006.

84. Martinez-Sanchez A, Alacid F, Rubio-Arias JA, Fernandez-Lobato B, Ramos-Campo DJ, Aguayo E. Consumption of Watermelon Juice Enriched in L-Citrulline and Pomegranate Ellagitannins Enhanced Metabolism during Physical Exercise. Journal of Agricultural and Food Chemistry. 2017;65(22):4395-404. doi: 10.1021/acs.jafc.7b00586. PubMed PMID: WOS:000403136600004.

85. Gonzales JU, Raymond A, Ashley J, Kim Y. Does l-citrulline supplementation improve exercise blood flow in older adults? Experimental physiology. 2017;102(12):1661-71. doi: 10.1113/ep086587. PubMed PMID: WOS:000416871800008.

86. Figueroa A, Wong A, Jaime SJ, Gonzales JU. Influence of l-citrulline and watermelon supplementation on vascular function and exercise performance. Current opinion in clinical nutrition and metabolic care. 2017;20(1):92-8. doi: 10.1097/mco.0000000000000340. PubMed PMID: WOS:000390242800013.

87. Suzuki T, Morita M, Kobayashi Y, Kamimura A. Oral L-citrulline supplementation enhances cycling time trial performance in healthy trained men: Double-blind randomized placebo-controlled 2-way crossover study. Journal of the International Society of Sports Nutrition. 2016;13. doi: 10.1186/s12970-016-0117-z. PubMed PMID: WOS:000370417200001.

88. Persson PB, Bondke Persson A. Nitric oxide: a classic revisited. Acta Physiologica. 2013;207(3):427-9. doi: 10.1111/apha.12052.

89. Sureda A, Pons A. Arginine and Citrulline Supplementation in Sports and Exercise: Ergogenic Nutrients? In: Lamprecht M, editor. Acute Topics in Sport Nutrition. Medicine and Sport Science. 592012. p. 18-28.

90. Bescos R, Sureda A, Tur JA, Pons A. The Effect of Nitric-Oxide-Related Supplements on Human Performance. Sports Medicine. 2012;42(2):99-117. doi: 10.2165/11596860-000000000-00000. PubMed PMID: WOS:000301093800002.

91. Flam BR, Eichler DC, Solomonson LP. Endothelial nitric oxide production is tightly coupled to the citrulline-NO cycle. Nitric Oxide. 2007;17(3-4):115-21. Epub 2007/09/18. doi: 10.1016/j.niox.2007.07.001. PubMed PMID: 17869551.

92. Jobgen WS, Fried SK, Fu WJ, Meininger CJ, Wu G. Regulatory role for the arginine–nitric oxide pathway in metabolism of energy substrates. The Journal of Nutritional Biochemistry. 2006;17(9):571-88. doi: https://doi.org/10.1016/j.jnutbio.2005.12.001.

93. Barbul A. Arginine: biochemistry, physiology, and therapeutic implications. JPEN Journal of parenteral and enteral nutrition. 1986;10(2):227-38. Epub 1986/03/01. doi: 10.1177/0148607186010002227. PubMed PMID: 3514981.

94. Palmer RM, Ashton DS, Moncada S. Vascular endothelial cells synthesize nitric oxide from L-arginine. Nature. 1988;333(6174):664-6. Epub 1988/06/16. doi: 10.1038/333664a0. PubMed PMID: 3131684.

95. Moncada S, Radomski MW, Palmer RM. Endothelium-derived relaxing factor. Identification as nitric oxide and role in the control of vascular tone and platelet function. Biochem Pharmacol. 1988;37(13):2495-501. Epub 1988/07/01. doi: 10.1016/0006-2952(88)90236-5. PubMed PMID: 3291879.

96. Bohlen HG. Nitric oxide and the cardiovascular system. Compr Physiol. 2015;5(2):808-23. Epub 2015/04/17. doi: 10.1002/cphy.c140052. PubMed PMID: 25880514.

97. Schwedhelm E, Maas R, Freese R, et al. Pharmacokinetic and pharmacodynamic properties of oral L-citrulline and L-arginine: impact on nitric oxide metabolism. British Journal of Clinical Pharmacology. 2008;65(1):51-9. doi: 10.1111/j.1365-2125.2007.02990.x.

98. Luiking YC, Deutz NE. Isotopic investigation of nitric oxide metabolism in disease. Current opinion in clinical nutrition and metabolic care. 2003;6(1):103-8. Epub 2002/12/24. doi: 10.1097/01.mco.0000049045.06038.79. PubMed PMID: 12496687.

99. Heys SD, Gardner E. Nutrients and the surgical patient: current and potential therapeutic applications to clinical practice. J R Coll Surg Edinb. 1999;44(5):283-93. PubMed PMID: 10550950.

100. Visek WJ. Arginine needs, physiological state and usual diets. A reevaluation. The Journal of nutrition. 1986;116(1):36-46. Epub 1986/01/01. doi: 10.1093/jn/116.1.36. PubMed PMID: 3080558.

101. Castillo L, Beaumier L, Ajami AM, Young VR. Whole body nitric oxide synthesis in healthy men determined from [15N] arginine-to-[15N]citrulline labeling. 1996;93(21):11460-5. doi: 10.1073/pnas.93.21.11460.

102. Dejong CH, Welters CF, Deutz NE, Heineman E, Soeters PB. Renal arginine metabolism in fasted rats with subacute short bowel syndrome. Clinical science. 1998;95(4):409-18. Epub 1998/09/28. PubMed PMID: 9748416.

103. Dhanakoti SN, Brosnan JT, Herzberg GR, Brosnan ME. Renal arginine synthesis: studies in vitro and in vivo. The American journal of physiology. 1990;259(3 Pt 1):E437-42. Epub 1990/09/01. doi: 10.1152/ajpendo.1990.259.3.E437. PubMed PMID: 1975989.

104. Featherston WR, Rogers QR, Freedland RA. Relative importance of kidney and liver in synthesis of arginine by the rat. The American journal of physiology. 1973;224(1):127-9. Epub 1973/01/01. doi: 10.1152/ajplegacy.1973.224.1.127. PubMed PMID: 4683290.

105. Ligthart-Melis GC, van de Poll MC, Boelens PG, Dejong CH, Deutz NE, van Leeuwen PA. Glutamine is an important precursor for de novo synthesis of arginine in humans. Am J Clin Nutr. 2008;87(5):1282-9. Epub 2008/05/13. doi: 10.1093/ajcn/87.5.1282. PubMed PMID: 18469251.

106. van de Poll MC, Siroen MP, van Leeuwen PA, et al. Interorgan amino acid exchange in humans: consequences for arginine and citrulline metabolism. Am J Clin Nutr. 2007;85(1):167-72. Epub 2007/01/09. doi: 10.1093/ajcn/85.1.167. PubMed PMID: 17209193.

107. van de Poll MC, Soeters PB, Deutz NE, Fearon KC, Dejong CH. Renal metabolism of amino acids: its role in interorgan amino acid exchange. Am J Clin Nutr. 2004;79(2):185-97. Epub 2004/01/30. doi: 10.1093/ajcn/79.2.185. PubMed PMID: 14749222.

108. Cynober L. Pharmacokinetics of arginine and related amino acids. The Journal of nutrition. 2007;137(6 Suppl 2):1646S-9S. Epub 2007/05/22. doi: 10.1093/jn/137.6.1646S. PubMed PMID: 17513441.

109. Morris SM. Arginine Metabolism: Boundaries of Our Knowledge. The Journal of nutrition. 2007;137(6):1602S-9S. doi: 10.1093/jn/137.6.1602s.

110. Wu G, Bazer FW, Davis TA, et al. Arginine metabolism and nutrition in growth, health and disease. Amino Acids. 2009;37(1):153-68. doi: 10.1007/s00726-008-0210-y.

111. Shin S, Mohan S, Fung HL. Intracellular L-arginine concentration does not determine NO production in endothelial cells: implications on the "L-arginine paradox". Biochem Biophys Res Commun. 2011;414(4):660-3. Epub 2011/10/12. doi: 10.1016/j.bbrc.2011.09.112. PubMed PMID: 21986532; PubMed Central PMCID: PMCPMC3210395.

112. Marini JC. Arginine and Ornithine Are the Main Precursors for Citrulline Synthesis in Mice. The Journal of nutrition. 2012;142(3):572-80. doi: 10.3945/jn.111.153825.

113. Ban H, Shigemitsu K, Yamatsuji T, et al. Arginine and Leucine regulate p70 S6 kinase and 4E-BP1 in intestinal epithelial cells. Int J Mol Med. 2004;13(4):537-43. Epub 2004/03/11. PubMed PMID: 15010853.

114. Bauchart-Thevret C, Cui L, Wu G, Burrin DG. Arginine-induced stimulation of protein synthesis and survival in IPEC-J2 cells is mediated by mTOR but not nitric oxide. 2010;299(6):E899-E909. doi: 10.1152/ajpendo.00068.2010.

115. Acworth I, Nicholass J, Morgan B, Newsholme EA. Effect of sustained exercise on concentrations of plasma aromatic and branched-chain amino acids and brain amines. 1986;137(1):149-53. doi: 10.1016/0006-291x(86)91188-5.

116. BLOMSTRAND E, CELSING F, NEWSHOLME EA. Changes in plasma concentrations of aromatic and branched-chain amino acids during sustained exercise in man and their possible role in fatigue. Acta Physiologica Scandinavica. 1988;133(1):115-21. doi: 10.1111/j.1748-1716.1988.tb08388.x.

117. Wilkinson DJ, Hossain T, Hill DS, et al. Effects of leucine and its metabolite β-hydroxy-β-methylbutyrate on human skeletal muscle protein metabolism. 2013;591(11):2911-23. doi: 10.1113/jphysiol.2013.253203.

118. Wolfe RR. Branched-chain amino acids and muscle protein synthesis in humans: myth or reality? J Int Soc Sports Nutr. 2017;14:30. Epub 2017/08/31. doi: 10.1186/s12970-017-0184-9. PubMed PMID: 28852372; PubMed Central PMCID: PMCPMC5568273.

119. Gleeson M. Interrelationship between physical activity and branched-chain amino acids. The Journal of nutrition. 2005;135(6 Suppl):1591S-5S. Epub 2005/06/03. doi: 10.1093/jn/135.6.1591S. PubMed PMID: 15930475.

120. Xiao Q, Moore SC, Keadle SK, et al. Objectively measured physical activity and plasma metabolomics in the Shanghai Physical Activity Study. International Journal of Epidemiology. 2016;45(5):1433-44. doi: 10.1093/ije/dyw033.

121. Yoneshiro T, Wang Q, Tajima K, et al. BCAA catabolism in brown fat controls energy homeostasis through SLC25A44. Nature. 2019. doi: 10.1038/s41586-019-1503-x.

122. Xu H, Gajda AM, Zhou YX, et al. Muscle metabolic reprogramming underlies the resistance of LFABP-null mice to high-fat feeding-induced decline in exercise capacity. J Biol Chem. 2019. Epub 2019/08/28. doi: 10.1074/jbc.RA118.006684. PubMed PMID: 31451493.

123. Neinast MD, Jang C, Hui S, et al. Quantitative Analysis of the Whole-Body Metabolic Fate of Branched-Chain Amino Acids. Cell Metabolism. 2019;29(2):417-29.e4. doi: 10.1016/j.cmet.2018.10.013.

124. Fedry J, Blais A, Even PC, et al. Urinary Metabolic Profile Predicts High Fat Diet Sensitivity in the C57Bl6/J mouse. The Journal of Nutritional Biochemistry. 2016. doi: 10.1016/j.jnutbio.2015.12.015.

125. Sunny NE, Kalavalapalli S, Bril F, et al. Cross-talk between branched-chain amino acids and hepatic mitochondria is compromised in nonalcoholic fatty liver disease. American journal of physiology Endocrinology and metabolism. 2015;309(4):E311-9. Epub 2015/06/11. doi: 10.1152/ajpendo.00161.2015. PubMed PMID: 26058864; PubMed Central PMCID: PMCPMC4537921.

126. Do TT, Hindlet P, Waligora-Dupriet AJ, et al. Disturbed intestinal nitrogen homeostasis in a mouse model of high-fat diet-induced obesity and glucose intolerance. American journal of physiology Endocrinology and metabolism. 2014;306(6):E668-80. doi: 10.1152/ajpendo.00437.2013. PubMed PMID: 24425764.

127. Kainulainen H, Hulmi JJ, Kujala UM. Potential Role of Branched-Chain Amino Acid Catabolism in Regulating Fat Oxidation. 2013;41(4):194-200. doi: 10.1097/jes.0b013e3182a4e6b6.

128. Holeček M. Branched-chain amino acids in health and disease: metabolism, alterations in blood plasma, and as supplements. Nutrition & Metabolism. 2018;15(1). doi: 10.1186/s12986-018-0271-1.

129. Ananieva EA, Wilkinson AC. Branched-chain amino acid metabolism in cancer. Current opinion in clinical nutrition and metabolic care. 2018;21(1):64-70. doi: 10.1097/mco.0000000000000430.

130. Rivera ME, Lyon ES, Vaughan RA. Effect of metformin on myotube BCAA catabolism. Journal of Cellular Biochemistry. 2019. doi: 10.1002/jcb.29327.

131. Tobias DK, Clish C, Mora S, et al. Dietary Intakes and Circulating Concentrations of Branched-Chain Amino Acids in Relation to Incident Type 2 Diabetes Risk Among High-Risk Women with a History of Gestational Diabetes Mellitus. Clinical chemistry. 2018;64(8):1203-10. doi: 10.1373/clinchem.2017.285841.

132. Blackburn P, Gass J, Pinto E Vairo F, et al. Maple syrup urine disease: mechanisms and management. The Application of Clinical Genetics. 2017;Volume 10:57-66. doi: 10.2147/tacg.s125962.

133. Mochel F, Duteil S, Marelli C, et al. Dietary anaplerotic therapy improves peripheral tissue energy metabolism in patients with Huntington's disease. 2010;18(9):1057-60. doi: 10.1038/ejhg.2010.72.

134. Roe CR, Mochel F. Anaplerotic diet therapy in inherited metabolic disease: Therapeutic potential. 2006;29(2-3):332-40. doi: 10.1007/s10545-006-0290-3.

135. Strauss KA, Puffenberger EG, Morton DH. Maple Syrup Urine Disease. In: Adam MP, Ardinger HH, Pagon RA, Wallace SE, Bean LJH, Stephens K, et al., editors. GeneReviews((R)). Seattle (WA): University of Washington, Seattle University of Washington, Seattle. GeneReviews is a registered trademark of the University of Washington, Seattle. All rights reserved.; 1993.

136. Houten SM, Herrema H, Te Brinke H, et al. Impaired amino acid metabolism contributes to fasting-induced hypoglycemia in fatty acid oxidation defects. Human molecular genetics. 2013;22(25):5249-61. doi: 10.1093/hmg/ddt382.

137. Adams SH, Hoppel CL, Lok KH, et al. Plasma Acylcarnitine Profiles Suggest Incomplete Long-Chain Fatty Acid -Oxidation and Altered Tricarboxylic Acid Cycle Activity in Type 2 Diabetic African-American Women. 2009;139(6):1073-81. doi: 10.3945/jn.108.103754.

138. Brunengraber H, Roe CR. Anaplerotic molecules: current and future. J Inherit Metab Dis. 2006;29(2-3):327-31. Epub 2006/06/10. doi: 10.1007/s10545-006-0320-1. PubMed PMID: 16763895.

139. Owen OE, Kalhan SC, Hanson RW. The Key Role of Anaplerosis and Cataplerosis for Citric Acid Cycle Function. Journal of Biological Chemistry. 2002;277(34):30409-12. doi: 10.1074/jbc.r200006200.

140. Acosta W, Meek TH, Schutz H, Dlugosz EM, Garland T. Preference for Western diet coadapts in High Runner mice and affects voluntary exercise and spontaneous physical activity in a genotype-dependent manner. Behavioural Processes. 2017;135:56-65. doi: https://doi.org/10.1016/j.beproc.2016.11.018.

141. Ruegsegger GN, Booth FW. Running from Disease: Molecular Mechanisms Associating Dopamine and Leptin Signaling in the Brain with Physical Inactivity, Obesity, and Type 2 Diabetes. Frontiers in Endocrinology. 2017;8. doi: 10.3389/fendo.2017.00109.

142. Zhou QY, Palmiter RD. Dopamine-deficient mice are severely hypoactive, adipsic, and aphagic. Cell. 1995;83(7):1197-209. Epub 1995/12/29. doi: 10.1016/0092-8674(95)90145-0. PubMed PMID: 8548806.

143. Salvatore MF, McInnis TR, Cantu MA, Apple DM, Pruett BS. Tyrosine Hydroxylase Inhibition in Substantia Nigra Decreases Movement Frequency. Mol Neurobiol. 2018. Epub 2018/07/30. doi: 10.1007/s12035-018-1256-9. PubMed PMID: 30056575.

144. Jenner P. Molecular mechanisms of L-DOPA-induced dyskinesia. Nature Reviews Neuroscience. 2008;9:665. doi: 10.1038/nrn2471.

145. Daubner SC, Le T, Wang S. Tyrosine hydroxylase and regulation of dopamine synthesis. Archives of Biochemistry and Biophysics. 2011;508(1):1-12. doi: 10.1016/j.abb.2010.12.017.

146. Fernstrom JD, Fernstrom MH. Tyrosine, Phenylalanine, and Catecholamine Synthesis and Function in the Brain. The Journal of nutrition. 2007;137(6):1539S-47S. doi: 10.1093/jn/137.6.1539s.

147. Mokdad AH. Actual Causes of Death in the United States, 2000. JAMA. 2004;291(10):1238. doi: 10.1001/jama.291.10.1238.

148. Lightfoot JT, Turner MJ, Daves M, Vordermark A, Kleeberger SR. Genetic influence on daily wheel running activity level. Physiological genomics. 2004;19(3):270-6. Epub 2004/09/24. doi: 10.1152/physiolgenomics.00125.2004. PubMed PMID: 15383638.

149. Turner MJ, Kleeberger SR, Lightfoot JT. Influence of genetic background on daily running-wheel activity differs with aging. Physiological genomics. 2005;22(1):76-85. Epub 2005/04/28. doi: 10.1152/physiolgenomics.00243.2004. PubMed PMID: 15855385.

150. Van Hove JLK, Saenz MS, Thomas JA, et al. Succinyl-CoA Ligase Deficiency: A Mitochondrial Hepatoencephalomyopathy. Pediatric Research. 2010;68(2):159-64. doi: 10.1203/pdr.0b013e3181e5c3a4.

151. Marini JC, Keller B, Didelija IC, Castillo L, Lee B. Enteral arginase II provides ornithine for citrulline synthesis. 2011;300(1):E188-E94. doi: 10.1152/ajpendo.00413.2010.

152. Marini JC, Didelija IC, Castillo L, Lee B. Glutamine: precursor or nitrogen donor for citrulline synthesis? 2010;299(1):E69-E79. doi: 10.1152/ajpendo.00080.2010.

153. Luiking YC, Engelen MP, Deutz NE. Regulation of nitric oxide production in health and disease. Current opinion in clinical nutrition and metabolic care. 2010;13(1):97-104. Epub 2009/10/21. doi: 10.1097/MCO.0b013e328332f99d. PubMed PMID: 19841582; PubMed Central PMCID: PMCPMC2953417.

154. Hallemeesch MM, Lamers WH, Deutz NEP. Reduced arginine availability and nitric oxide production. Clinical Nutrition. 2002;21(4):273-9. doi: 10.1054/clnu.2002.0571.

155. Engelen MP, Safar AM, Bartter T, Koeman F, Deutz NE. Reduced arginine availability and nitric oxide synthesis in cancer is related to impaired endogenous arginine synthesis. Clinical science. 2016;130(14):1185-95. Epub 2016/04/30. doi: 10.1042/CS20160233. PubMed PMID: 27129191.

156. Kojda G, Cheng YC, Burchfield J, Harrison DG. Dysfunctional Regulation of Endothelial Nitric Oxide Synthase (eNOS) Expression in Response to Exercise in Mice Lacking One eNOS Gene. 2001;103(23):2839-44. doi: 10.1161/01.cir.103.23.2839.

157. Momken I, Lechene P, Ventura-Clapier R, Veksler V. Voluntary physical activity alterations in endothelial nitric oxide synthase knockout mice. Am J Physiol Heart Circ Physiol. 2004;287(2):H914-20. Epub 2004/07/28. doi: 10.1152/ajpheart.00651.2003. PubMed PMID: 15277206.

158. Momken I, Fortin D, Serrurier B, Bigard X, Ventura-Clapier R, Veksler V. Endothelial nitric oxide synthase (NOS) deficiency affects energy metabolism pattern in murine oxidative skeletal muscle. 2002;368(1):341-7. doi: 10.1042/bj20020591.

159. Wolfe R. A Guide to Amino Acid and Protein Nutrition: Essential Amino Acid Solutions for Everyone (the EAASE Program): Independently Published; 2017.

160. Hallemeesch MM, Ten Have GA, Deutz NE. Metabolic flux measurements across portal drained viscera, liver, kidney and hindquarter in mice. Lab Anim. 2001;35(1):101-10. Epub 2001/02/24. doi: 10.1258/0023677011911426. PubMed PMID: 11201286.

161. Jonker R, Deutz NEP, Ligthart-Melis GC, et al. Preserved anabolic threshold and capacity as estimated by a novel stable tracer approach suggests no anabolic resistance or increased requirements in weight stable COPD patients. Clin Nutr. 2019. Epub 2018/08/14. doi: 10.1016/j.clnu.2018.07.018. PubMed PMID: 30100106.

162. Deutz NEP, Ashurst I, Ballesteros MD, et al. The Underappreciated Role of Low Muscle Mass in the Management of Malnutrition. Journal of the American Medical Directors Association. 2019;20(1):22-7. doi: https://doi.org/10.1016/j.jamda.2018.11.021.

163. Jonker R, Deutz NEP, Harrykissoon R, Zachria AJ, Veley EA, Engelen M. A critical evaluation of the anabolic response after bolus or continuous feeding in COPD and healthy older adults. Clinical science. 2018;132(1):17-31. Epub 2017/12/01. doi: 10.1042/CS20171068. PubMed PMID: 29187513.

164. Hallemeesch M, Soeters P, Deutz N. In vivo whole body nitric oxide synthesis, determined by the conversion of [15N2]arginine to [15N]citrulline, is not increased in acute endotoxin-treated mice. Faseb Journal. 1999;13(4):A103-A. PubMed PMID: WOS:000082033300594.

165. Soeters PB, Hallemeesch MM, Bruins MJ, van Eijk HM, Deutz NE. Quantitative in vivo assessment of arginine utilization and nitric oxide production in endotoxemia. American journal of surgery. 2002;183(4):480-8. Epub 2002/04/27. doi: 10.1016/S0002-9610(02)00847-4. PubMed PMID: 11975939.

166. Hallemeesch MM, Vissers YL, Soeters PB, Deutz NE. Acute reduction of circulating arginine in mice does not compromise whole body NO production. Clin Nutr. 2004;23(3):383-90. Epub 2004/05/26. doi: 10.1016/j.clnu.2003.09.003. PubMed PMID: 15158302.

167. da Silva RP, Nissim I, Brosnan ME, Brosnan JT. Creatine synthesis: hepatic metabolism of guanidinoacetate and creatine in the rat in vitro and in vivo. American journal of physiology Endocrinology and metabolism. 2009;296(2):E256-E61. Epub 2008/11/18. doi: 10.1152/ajpendo.90547.2008. PubMed PMID: 19017728.

168. Deutz NE. The 2007 ESPEN Sir David Cuthbertson Lecture: amino acids between and within organs. The glutamate-glutamine-citrulline-arginine pathway. Clin Nutr. 2008;27(3):321-7. Epub 2008/05/27. doi: 10.1016/j.clnu.2008.03.010. PubMed PMID: 18501998.

169. Vissers YL, von Meyenfeldt MF, Luiking YC, Dejong CH, Buurman WA, Deutz NE. Presence of tumour inhibits the normal post-operative response in arginine and NO production in non-cachectic mice. Clinical science. 2007;112(10):527-32. Epub 2007/01/11. doi: 10.1042/CS20060340. PubMed PMID: 17212586.

170. Yelamanchi SD, Jayaram S, Thomas JK, et al. A pathway map of glutamate metabolism. Journal of Cell Communication and Signaling. 2016;10(1):69-75. doi: 10.1007/s12079-015-0315-5.

171. Luiking YC, Steens L, Poeze M, Ramsay G, Deutz NEP. Low plasma arginine concentration in septic patients is related to diminished de novo arginine production from citrulline. Clinical Nutrition. 2003;22(S1):S26.

172. Hallemeesch MM, Janssen BJ, de Jonge WJ, Soeters PB, Lamers WH, Deutz NE. NO production by cNOS and iNOS reflects blood pressure changes in LPS-challenged mice. American journal of physiology Endocrinology and metabolism. 2003;285(4):E871-5. Epub 2003/05/02. doi: 10.1152/ajpendo.00004.2002. PubMed PMID: 12721155.

173. Hallemeesch MM, Cobben DC, Dejong CH, Soeters PB, Deutz NE. Renal amino acid metabolism during endotoxemia in the rat. The Journal of surgical research. 2000;92(2):193-200. Epub 2000/07/18. doi: 10.1006/jsre.2000.5867. PubMed PMID: 10896821.

174. Hallemeesch MM, Cobben DCP, Deutz NEP, Soeters PB. Reduced gut citrulline production does not lead to reduced renal arginine production after endotoxin treatment in the rat. Gastroenterology. 1998;114(4):A882. doi: 10.1016/s0016-5085(98)83591-9. PubMed PMID: WOS:000073089603590.

175. Van Acker BA, Hulsewe KW, Wagenmakers AJ, et al. Absence of glutamine isotopic steady state: implications for the assessment of whole-body glutamine production rate. Clinical science. 1998;95(3):339-46. Epub 1998/09/09. PubMed PMID: 9730854.

176. Blomstrand E, Hassmen P, Ekblom B, Newsholme EA. Administration of branched-chain amino acids during sustained exercise - effects on performance and on plasma concentration of some amino acids. European Journal of Applied Physiology and Occupational Physiology. 1991;63(2):83-8. doi: 10.1007/bf00235174.

177. Verger P, Aymard P, Cynobert L, Anton G, Luigi R. Effects of administration of branched-chain amino acids vs. glucose during acute exercise in the rat. 1994;55(3):523-6. doi: 10.1016/0031-9384(94)90111-2.

178. Falavigna G, Junior J, Rogero M, et al. Effects of Diets Supplemented with Branched-Chain Amino Acids on the Performance and Fatigue Mechanisms of Rats Submitted to Prolonged Physical Exercise. Nutrients. 2012;4(11):1767-80. doi: 10.3390/nu4111767.

179. Kim D-H, Kim S-H, Jeong W-S, Lee H-Y. Effect of BCAA intake during endurance exercises on fatigue substances, muscle damage substances, and energy metabolism substances. Journal of Exercise Nutrition and Biochemistry. 2013;17(4):169-80. doi: 10.5717/jenb.2013.17.4.169.

180. Cheng IS, Wang YW, Chen IF, Hsu GS, Hsueh CF, Chang CK. The Supplementation of Branched-Chain Amino Acids, Arginine, and Citrulline Improves Endurance Exercise Performance in Two Consecutive Days. Journal of sports science & medicine. 2016;15(3):509-15. Epub 2016/11/03. PubMed PMID: 27803630; PubMed Central PMCID: PMCPMC4974864.

181. Hsueh C-F, Wu H-J, Tsai T-S, Wu C-L, Chang C-K. The Effect of Branched-Chain Amino Acids, Citrulline, and Arginine on High-Intensity Interval Performance in Young Swimmers. Nutrients. 2018;10(12):1979. doi: 10.3390/nu10121979.

182. Kato H, Suzuki K, Bannai M, Moore DR. Branched-Chain Amino Acids Are the Primary Limiting Amino Acids in the Diets of Endurance-Trained Men after a Bout of Prolonged Exercise. The Journal of nutrition. 2018;148(6):925-31. doi: 10.1093/jn/nxy048.

183. Bahadorani M, Tavalaee M, Abedpoor N, Ghaedi K, Nazem MN, Nasr-Esfahani MH. Effects of branched-chain amino acid supplementation and/or aerobic exercise on mouse sperm quality and testosterone production. Andrologia. 2019;51(2):e13183. doi: 10.1111/and.13183.

184. Lysenko EA, Vepkhvadze TF, Lednev EM, Vinogradova OL, Popov DV. Branched-chain amino acids administration suppresses endurance exercise-related activation of ubiquitin proteasome signaling in trained human skeletal muscle. The journal of physiological sciences : JPS. 2018;68(1):43-53. Epub 2016/12/04. doi: 10.1007/s12576-016-0506-8. PubMed PMID: 27913948.

185. Xu M, Kitaura Y, Ishikawa T, et al. Endurance performance and energy metabolism during exercise in mice with a muscle-specific defect in the control of branched-chain amino acid catabolism. PloS one. 2017;12(7):e0180989. doi: 10.1371/journal.pone.0180989.

186. Moura CS, Lollo PCB, Morato PN, Risso EM, Amaya-Farfan J. Modulatory effects of arginine, glutamine and branched-chain amino acids on heat shock proteins, immunity and antioxidant response in exercised rats. Food & function. 2017;8(9):3228-38. Epub 2017/08/16. doi: 10.1039/c7fo00465f. PubMed PMID: 28812766.

187. De Araujo JA, Falavigna G, Rogero MM, et al. Effect of chronic supplementation with branched-chain amino acids on the performance and hepatic and muscle glycogen content in trained rats. 2006;79(14):1343-8. doi: 10.1016/j.lfs.2006.03.045.

188. Coombes JS, McNaughton LR. Effects of branched-chain amino acid supplementation on serum creatine kinase and lactate dehydrogenase after prolonged exercise. J Sports Med Phys Fitness. 2000;40(3):240-6. Epub 2000/12/28. PubMed PMID: 11125767.

189. Calders P, Pannier JL, Matthys DM, Lacroix EM. Pre-exercise branched-chain amino acid administration increases endurance performance in rats. Medicine and science in sports and exercise. 1997;29(9):1182-6. doi: 10.1097/00005768-199709000-00010. PubMed PMID: 9309629.

190. Foure A, Nosaka K, Gastaldi M, et al. Effects of branched-chain amino acids supplementation on both plasma amino acids concentration and muscle energetics changes resulting from muscle damage: A randomized placebo controlled trial. Clin Nutr. 2016;35(1):83-94. Epub 2015/04/19. doi: 10.1016/j.clnu.2015.03.014. PubMed PMID: 25886707.

191. Shimomura Y, Murakami T, Nakai N, Nagasaki M, Harris RA. Exercise Promotes BCAA Catabolism: Effects of BCAA Supplementation on Skeletal Muscle during Exercise. The Journal of nutrition. 2004;134(6):1583S-7S. doi: 10.1093/jn/134.6.1583s.

192. Moberg M, Apró W, Ekblom B, Van Hall G, Holmberg H-C, Blomstrand E. Activation of mTORC1 by leucine is potentiated by branched-chain amino acids and even more so by essential amino acids following resistance exercise. 2016;310(11):C874-C84. doi: 10.1152/ajpcell.00374.2015.

193. Blomstrand E, Eliasson J, Karlsson HK, Kohnke R. Branched-chain amino acids activate key enzymes in protein synthesis after physical exercise. The Journal of nutrition. 2006;136(1 Suppl):269S-73S. Epub 2005/12/21. doi: 10.1093/jn/136.1.269S. PubMed PMID: 16365096.

194. Rennie MJ, Bohé J, Smith K, Wackerhage H, Greenhaff P. Branched-Chain Amino Acids as Fuels and Anabolic Signals in Human Muscle. The Journal of nutrition. 2006;136(1):264S-8S. doi: 10.1093/jn/136.1.264s.

195. Engelen MP, Rutten EP, De Castro CL, Wouters EF, Schols AM, Deutz NE. Supplementation of soy protein with branched-chain amino acids alters protein metabolism in healthy elderly and even more in patients with chronic obstructive pulmonary disease. Am J Clin Nutr. 2007;85(2):431-9. Epub 2007/02/08. doi: 10.1093/ajcn/85.2.431. PubMed PMID: 17284740.

196. Fuchs CJ, Hermans WJH, Holwerda AM, et al. Branched-chain amino acid and branched-chain ketoacid ingestion increases muscle protein synthesis rates in vivo in older adults: a double-blind, randomized trial. The American Journal of Clinical Nutrition. 2019. doi: 10.1093/ajcn/nqz120.

197. Jackman SR, Witard OC, Philp A, Wallis GA, Baar K, Tipton KD. Branched-Chain Amino Acid Ingestion Stimulates Muscle Myofibrillar Protein Synthesis following Resistance Exercise in Humans. Frontiers in physiology. 2017;8:390. Epub 2017/06/24. doi: 10.3389/fphys.2017.00390. PubMed PMID: 28638350; PubMed Central PMCID: PMCPMC5461297.

198. Ferreira MP, Li R, Cooke M, Kreider RB, Willoughby DS. Periexercise coingestion of branched-chain amino acids and carbohydrate in men does not preferentially augment resistance exercise-induced increases in phosphatidylinositol 3 kinase/protein kinase B-mammalian target of rapamycin pathway markers indicative of muscle protein synthesis. Nutr Res. 2014;34(3):191-8. Epub 2014/03/25. doi: 10.1016/j.nutres.2013.12.007. PubMed PMID: 24655485.

199. Louard RJ, Barrett EJ, Gelfand RA. Effect of infused branched-chain amino acids on muscle and whole-body amino acid metabolism in man. Clinical science. 1990;79(5):457-66. Epub 1990/11/01. doi: 10.1042/cs0790457. PubMed PMID: 2174312.

200. Frexes-Steed M, Lacy DB, Collins J, Abumrad NN. Role of leucine and other amino acids in regulating protein metabolism in vivo. The American journal of physiology. 1992;262(6 Pt 1):E925-35. Epub 1992/06/01. doi: 10.1152/ajpendo.1992.262.6.E925. PubMed PMID: 1616025.

201. Matthews DE. Observations of branched-chain amino acid administration in humans. The Journal of nutrition. 2005;135(6 Suppl):1580S-4S. Epub 2005/06/03. doi: 10.1093/jn/135.6.1580S. PubMed PMID: 15930473; PubMed Central PMCID: PMCPMC2268017.

202. Des Rosiers C, Labarthe F, Lloyd SG, Chatham JC. Cardiac anaplerosis in health and disease: food for thought. 2011;90(2):210-9. doi: 10.1093/cvr/cvr055.

203. Halarnkar PP, Blomquist GJ. Comparative aspects of propionate metabolism. Comparative Biochemistry and Physiology Part B: Comparative Biochemistry. 1989;92(2):227-31. doi: https://doi.org/10.1016/0305-0491(89)90270-8.

204. Eric Newsholme AL. Functional Biochemistry in Health and Disease: John Wiley & Sons; 2011. 543 p.

205. Wongkittichote P, Ah Mew N, Chapman KA. Propionyl-CoA carboxylase - A review. Mol Genet Metab. 2017;122(4):145-52. Epub 2017/10/17. doi: 10.1016/j.ymgme.2017.10.002. PubMed PMID: 29033250; PubMed Central PMCID: PMCPMC5725275.

206. Johnson JD, Muhonen WW, Lambeth DO. Characterization of the ATP- and GTP-specific Succinyl-CoA Synthetases in Pigeon: THE ENZYMES INCORPORATE THE SAME -SUBUNIT. 1998;273(42):27573-9. doi: 10.1074/jbc.273.42.27573.

207. Johnson JD, Mehus JG, Tews K, Milavetz BI, Lambeth DO. Genetic Evidence for the Expression of ATP- and GTP-specific Succinyl-CoA Synthetases in Multicellular Eucaryotes. Journal of Biological Chemistry. 1998;273(42):27580-6. doi: 10.1074/jbc.273.42.27580.

208. Ferguson DP, Schmitt EE, Lightfoot JT. Vivo-morpholinos induced transient knockdown of physical activity related proteins. PloS one. 2013;8(4):e61472. Epub 2013/05/01. doi: 10.1371/journal.pone.0061472. PubMed PMID: 23630592; PubMed Central PMCID: PMCPMC3632599.

209. Rendeiro C, Masnik AM, Mun JG, et al. Fructose decreases physical activity and increases body fat without affecting hippocampal neurogenesis and learning relative to an isocaloric glucose diet. Sci Rep. 2015;5:9589. doi: 10.1038/srep09589. PubMed PMID: 25892667.

210. Yeaman SJ. The 2-oxo acid dehydrogenase complexes: recent advances. 1989;257(3):625-32. doi: 10.1042/bj2570625.

211. Burch JS, Marcero JR, Maschek JA, et al. Glutamine via α-ketoglutarate dehydrogenase provides succinyl-CoA for heme synthesis during erythropoiesis. Blood. 2018;132(10):987-98. Epub 2018/07/10. doi: 10.1182/blood-2018-01-829036. PubMed PMID: 29991557.

212. Pasiakos SM. Exercise and amino acid anabolic cell signaling and the regulation of skeletal muscle mass. Nutrients. 2012;4(7):740-58. Epub 2012/08/02. doi: 10.3390/nu4070740. PubMed PMID: 22852061; PubMed Central PMCID: PMCPMC3407992.

213. Meesters RJ, Wolfe RR, Deutz NE. Application of liquid chromatography-tandem mass spectrometry (LC-MS/MS) for the analysis of stable isotope enrichments of phenylalanine and tyrosine. Journal of chromatography B, Analytical technologies in the biomedical and life sciences. 2009;877(1-2):43-9. Epub 2008/11/28. doi: 10.1016/j.jchromb.2008.11.018. PubMed PMID: 19036645.

214. van der Meij BS, Deutz NEP, Rodriguez RER, Engelen M. Increased amino acid turnover and myofibrillar protein breakdown in advanced cancer are associated with muscle weakness and impaired physical function. Clin Nutr. 2018. Epub 2018/11/28. doi: 10.1016/j.clnu.2018.10.022. PubMed PMID: 30477932.

215. Bernheimer H, Birkmayer W, Hornykiewicz O, Jellinger K, Seitelberger F. Brain dopamine and the syndromes of Parkinson and Huntington Clinical, morphological and neurochemical correlations. Journal of the Neurological Sciences. 1973;20(4):415-55. doi: 10.1016/0022-510X(73)90175-5.

216. Moinard C, Tliba L, Diaz J, et al. Citrulline stimulates locomotor activity in aged rats: Implication of the dopaminergic pathway. Nutrition. 2017;38:9-12. doi: 10.1016/j.nut.2017.01.001. PubMed PMID: WOS:000402224000004.

217. Friend DM, Devarakonda K, O'Neal TJ, et al. Basal Ganglia Dysfunction Contributes to Physical Inactivity in Obesity. Cell Metab. 2017;25(2):312-21. Epub 2017/01/04. doi: 10.1016/j.cmet.2016.12.001. PubMed PMID: 28041956; PubMed Central PMCID: PMCPMC5299005.

218. Roe CR, Mochel F. Anaplerotic diet therapy in inherited metabolic disease: therapeutic potential. J Inherit Metab Dis. 2006;29(2-3):332-40. Epub 2006/06/10. doi: 10.1007/s10545-006-0290-3. PubMed PMID: 16763896.

219. Vissers YL, von Meyenfeldt MF, Argiles JM, Luiking YC, Dejong CH, Deutz NE. Protein breakdown on whole-body and organ level in non-cachectic tumour-bearing mice undergoing surgery. Clin Nutr. 2007;26(4):483-90. Epub 2007/05/22. doi: 10.1016/j.clnu.2007.03.005. PubMed PMID: 17513024.

220. Vissers YL, von Meyenfeldt MF, Braulio VB, Luiking YC, Deutz NE. Measuring whole-body actin/myosin protein breakdown in mice using a primed constant stable isotope-infusion protocol. Clinical science. 2003;104(6):585-90. Epub 2003/02/19. doi: 10.1042/CS20020283. PubMed PMID: 12589703.

221. van Eijk HM, Deutz NE, Wagenmakers AJ, Soeters PB. 3-Methylhistidine determined in plasma by "high-performance" lipid chromatography. Clinical chemistry. 1990;36(3):556-9. Epub 1990/03/01. PubMed PMID: 2311233.

222. Tipton KD, Hamilton DL, Gallagher IJ. Assessing the Role of Muscle Protein Breakdown in Response to Nutrition and Exercise in Humans. Sports medicine (Auckland, NZ). 2018;48(Suppl 1):53-64. Epub 2018/01/26. doi: 10.1007/s40279-017-0845-5. PubMed PMID: 29368185; PubMed Central PMCID: PMCPMC5790854.

223. Rutten EP, Franssen FM, Engelen MP, Wouters EF, Deutz NE, Schols AM. Greater whole-body myofibrillar protein breakdown in cachectic patients with chronic obstructive pulmonary disease. Am J Clin Nutr. 2006;83(4):829-34. Epub 2006/04/08. doi: 10.1093/ajcn/83.4.829. PubMed PMID: 16600935.

224. Rutten EPA, Engelen MPKJ, Wouters EFM, Deutz NEP, Schols AMWJ. Reduced myofibrillar protein breakdown in stable, patients with chronic obstructive pulmonary disease (COPD). Faseb Journal. 2004;18(4):A540-A. PubMed PMID: WOS:000220470602597.

APPENDIX A

FIGURES

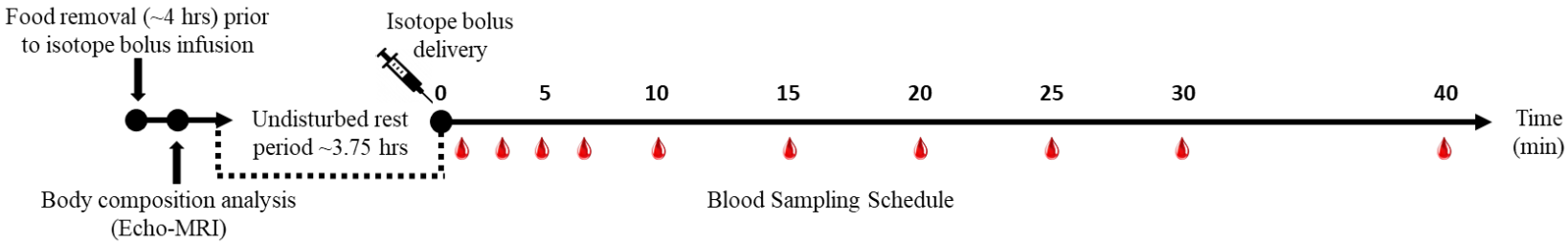

Figure 1 - Study Timeline: Study timeline depicts procedures performed prior to and following isotope bolus delivery. Blood sampling times are depicted by blood drop images at (1, 3, 5, 7, 10, 15, 20, 30, & 40 mins).

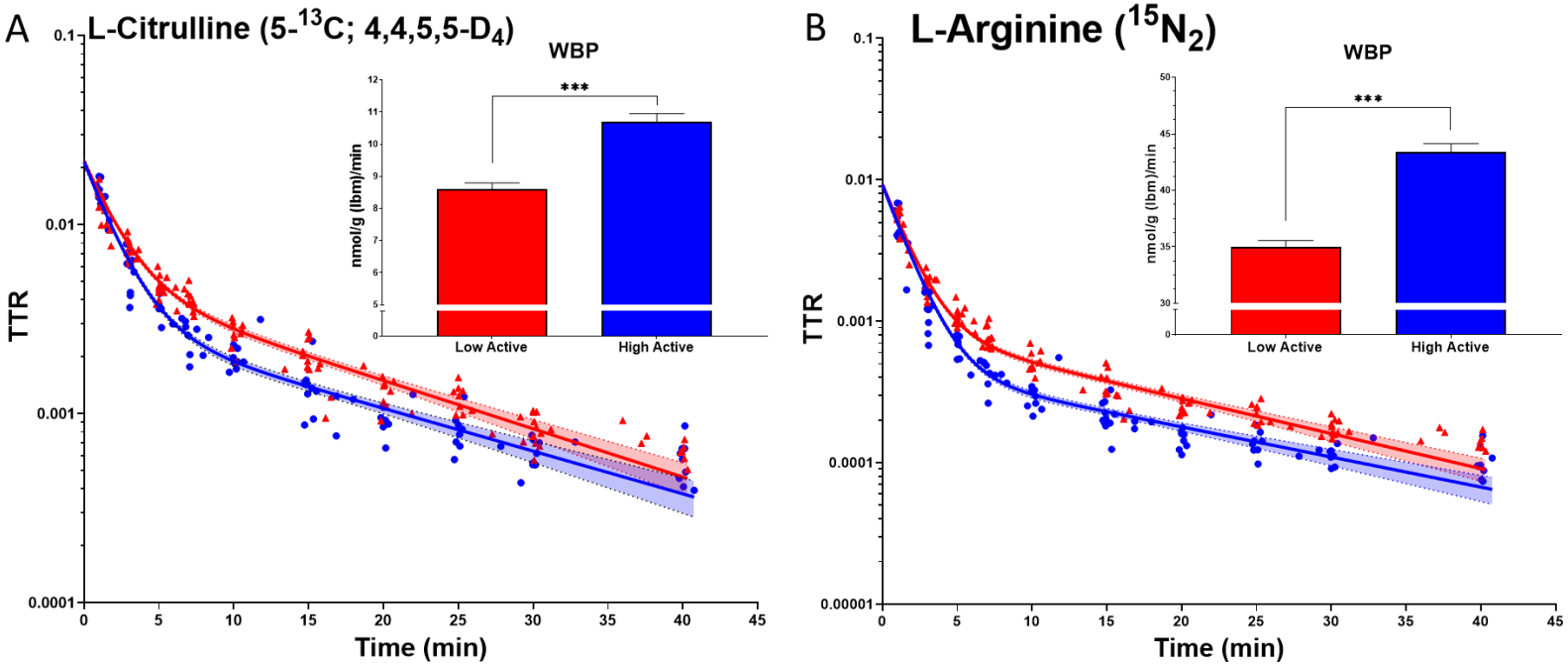

Figure 2- Citrulline & Arginine Whole-Body Production: Logarithmic fitting of tracer-tracee ratio (TTR) of L-Citrulline [5-^{13}C; 4,4,5,5-D_4] (panel A) and L-Arginine [Guanidino-$^{15}N_2$] (panel B) in low-active (gray) and high-active (black) mice over a period of 40 mins. The fit was utilized for calculations of citrulline and arginine whole-body production (WBP) depicted in bar graphs. Data are normalized for lean body mass (lbm) and expressed as mean (± SE). Statistics are by t-test, *** indicates $p \leq 0.001$.

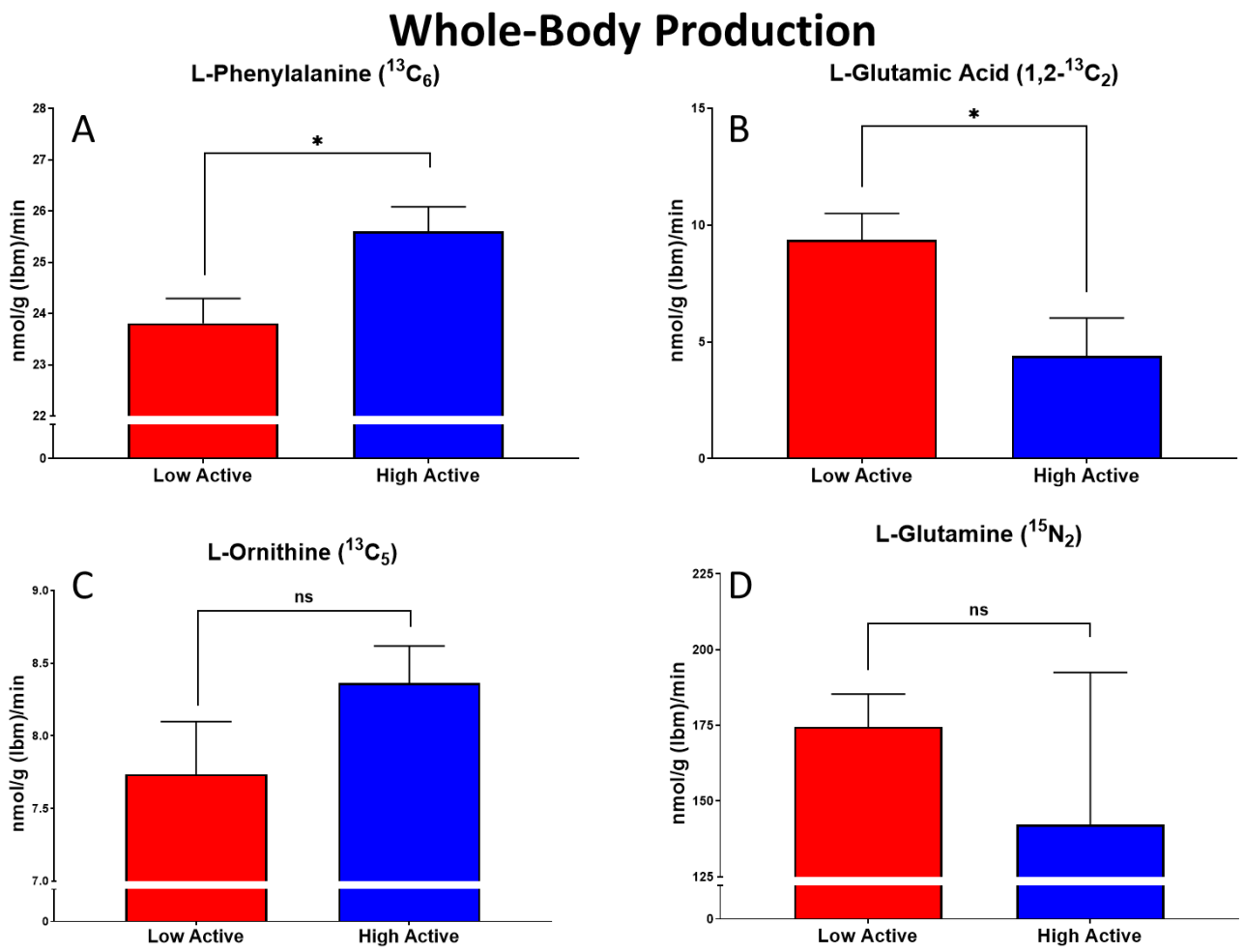

Figure 3 - Whole-Body Production of ARG Metabolites: Whole-body production (WBP) of L-Phenylalanine [Ring-$^{13}C_6$)] (panel A), L-Glutamic Acid [1,2-$^{13}C_2$] (panel B), L-Ornithine [$^{13}C_5$] (panel C), and L-Glutamine [$^{15}N_2$] (panel D) in low- and high-active mice. WBP was calculated from data collected over a 40 min period, normalized for lean body mass (lbm), and expressed as mean (± SE). Statistics are by t-test, * indicates $p \leq 0.05$.

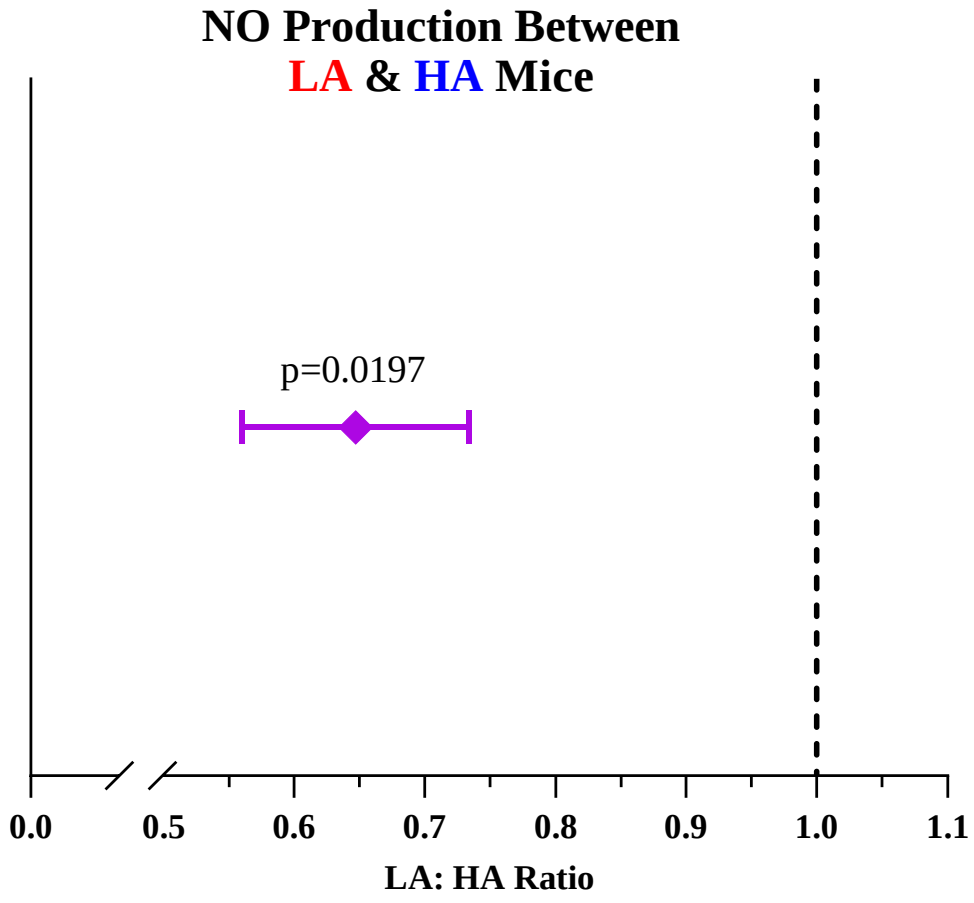

Figure 4 - Nitric Oxide Production Ratio: Nitric oxide (NO) production ratio between low- (LA) and high-active (HA) mice. Data are expressed as mean (± 95% CI). Statistics are by t-test with alpha level set at $p \leq 0.05$.

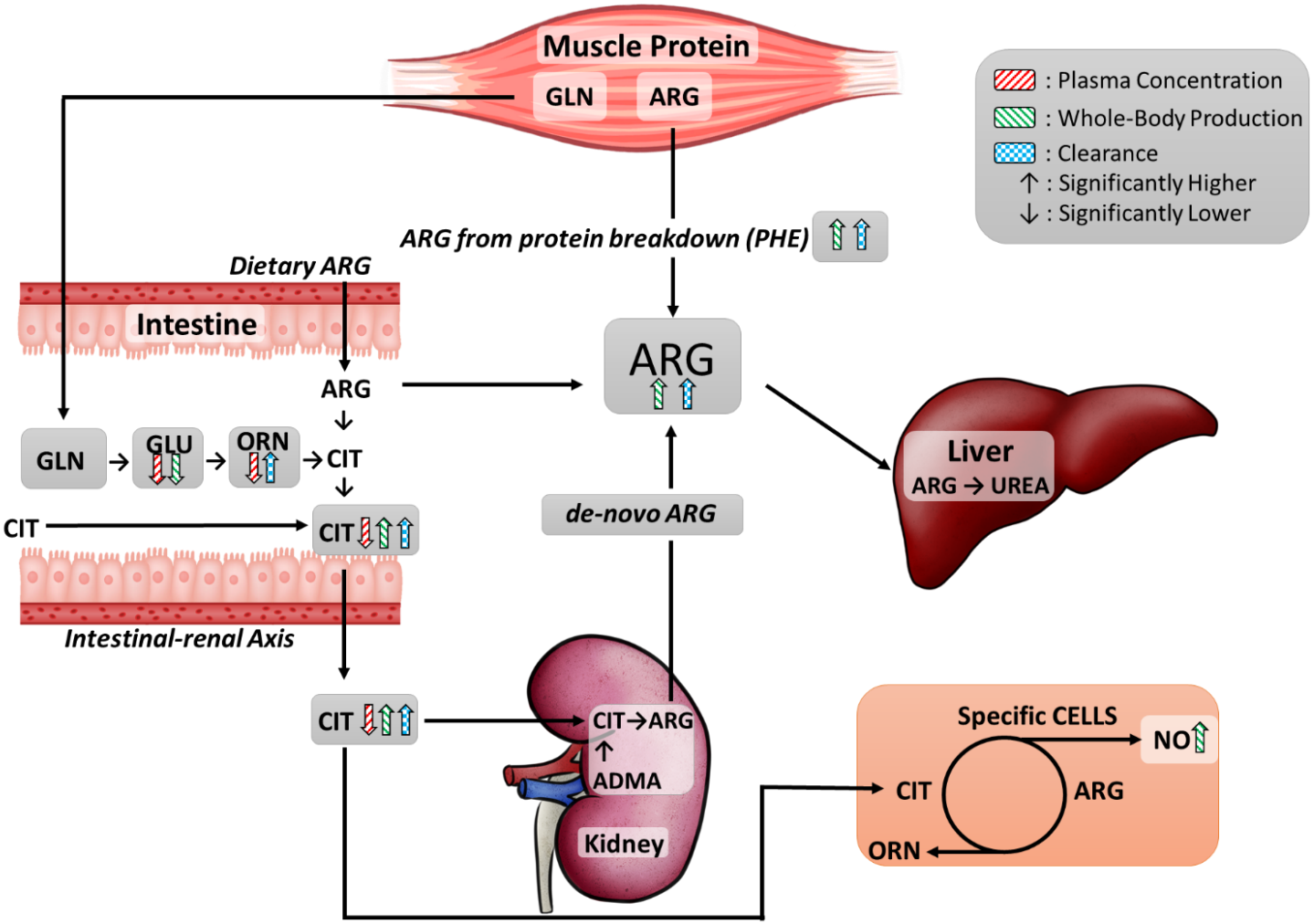

Figure 5 - Arginine Metabolic Pathway: Overview of activated whole-body arginine metabolic pathway in high-active mice compared to low-active mice. The direction of arrows depicts significantly higher or lower plasma concertation (red striped), whole-body production (green striped), or clearance (blue checkered) for ARG, CIT, ORN, GLN, GLU, PHE and NO. A lack of arrow within an amino acid or NO signifies no differences between mice.

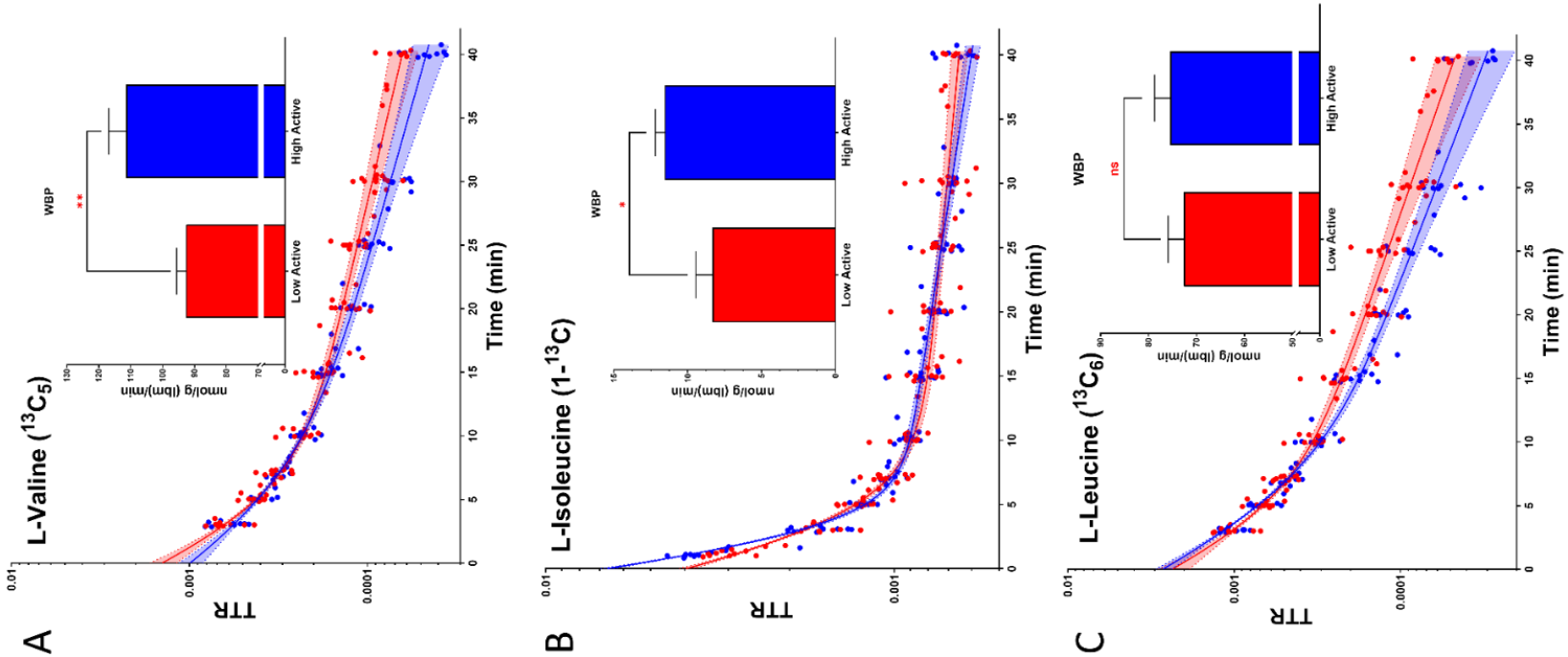

Figure 6 - TTR and Whole-Body Production of BCAA: Logarithmic fitting of tracer-tracee ratio (TTR) and whole-body production (WBP) of L-Valine ($^{13}C_5$) [panel A], L-Isoleucine (1-^{13}C) [panel B], and L-Leucine ($^{13}C_6$) [panel C] in low-active (red) and high-active (blue) mice over a period of 40 mins. Data are normalized for lean body mass (lbm) and expressed as mean (± 95% CI) for TTR log fit and mean (± SE) for WBP. Statistics are by *t*-test with alpha level set at * $p \leq 0.05$, ** indicates $p \leq 0.01$, and ns indicates no significance.

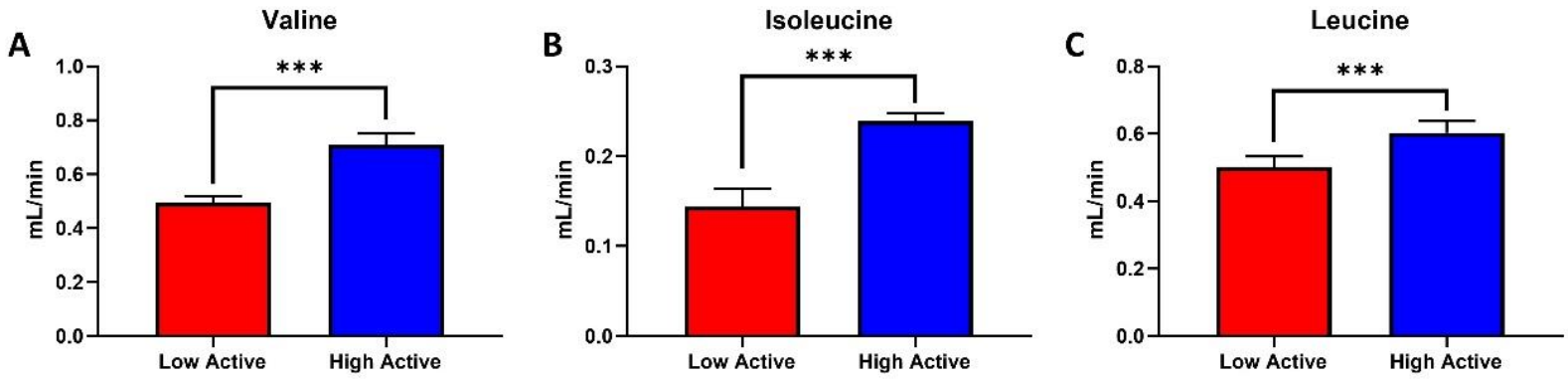

Figure 7 - BCAA Clearance Rates: Total clearance rate for valine ($^{13}C_5$) (panel A), isoleucine (1-^{13}C), and leucine ($^{13}C_6$) in low-active (red) and high-active (blue) mice over a period of 40 mins Clearance data was calculated as (whole-body production/plasma concentration) and expressed as mean (± SE). Statistics are by *t*-test, *** indicates $p \leq 0.001$.

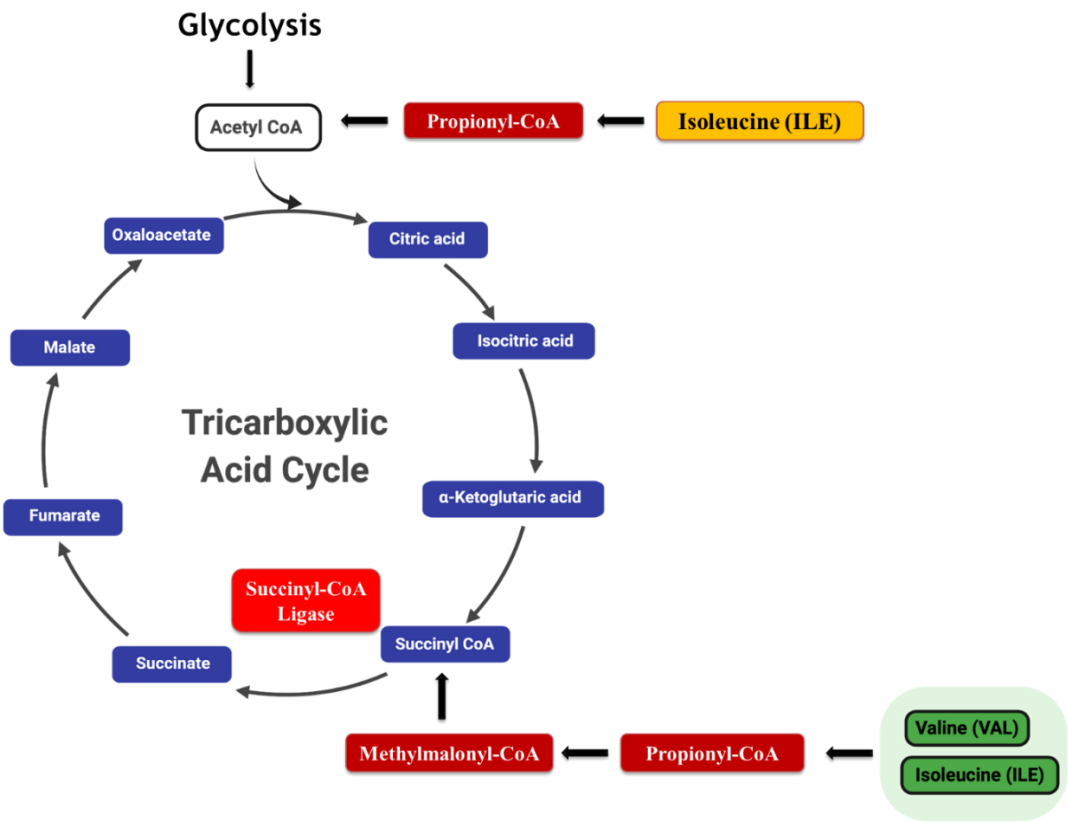

Figure 8 - Anaplerosis *via* Valine and Isoleucine: Overview of valine (VAL) and isoleucine (ILE) anaplerotic (replenishing) pathways of the TCA cycle. Green boxes represent VAL's and ILE's glucogenic pathway, while yellow depicts ILE's ketogenic pathway.

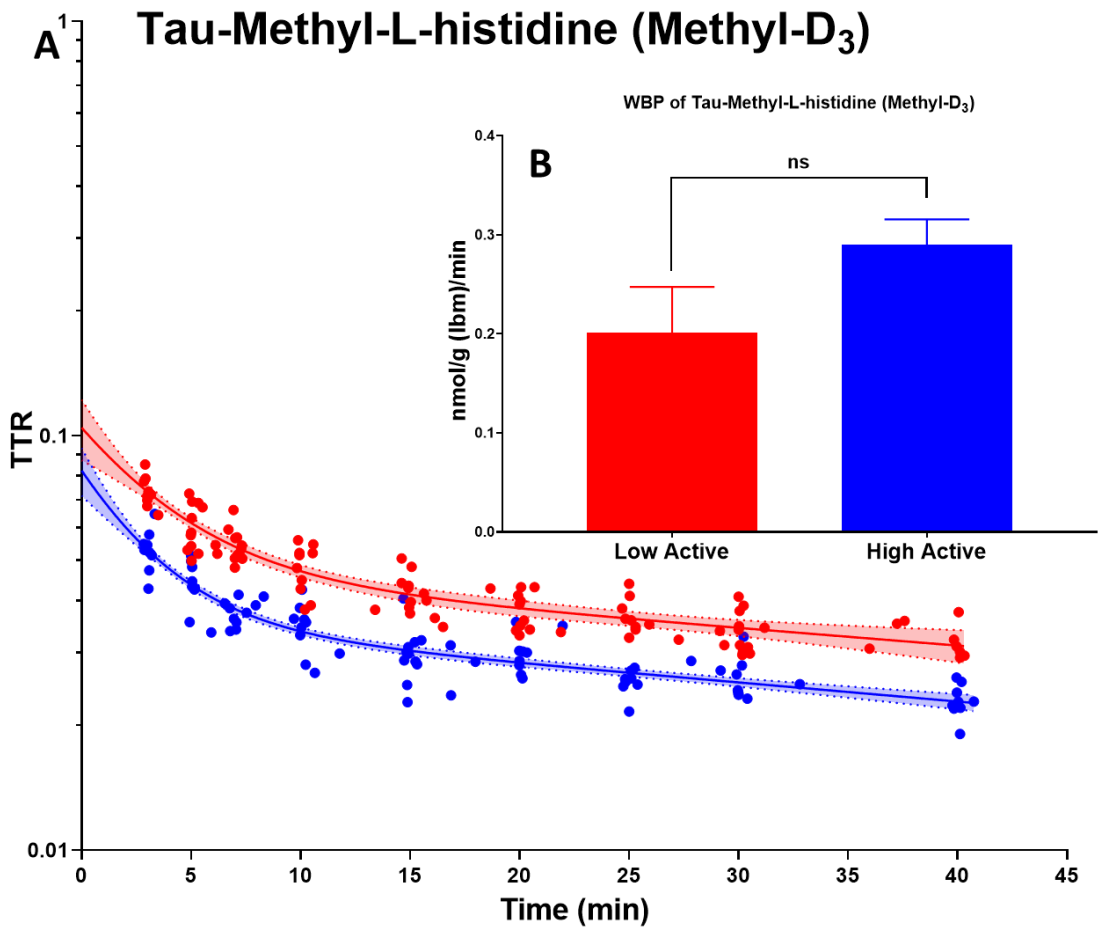

Figure 9 - TTR & Whole-Body Production of Tau-Methyl-Histidine: Logarithmic fitting of tracer-tracee ratio (TTR) [panel A] used to calculate whole-body production (WBP) of Tau-Methyl-L-Histidine [Methyl-D_3] (panel B) in low- and high-active mice over a period of 40 mins. Data are normalized for lean body mass (lbm) and expressed as mean (± 95% CI; panel A) and mean (± SE; panel B). Statistics are by t-test with alpha level set at $p \leq 0.05$.

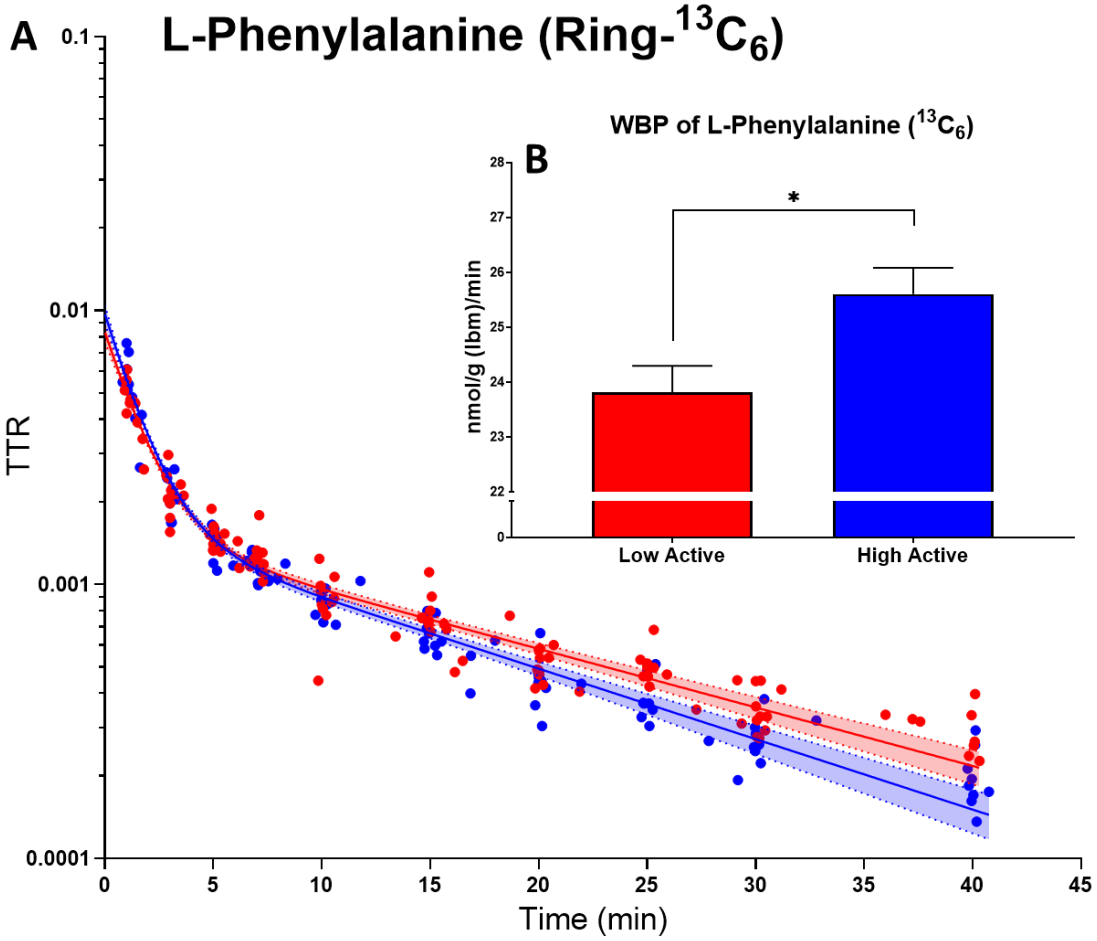

Figure 10 - Phenylalanine TTR & Whole-Body Production: Logarithmic fitting of tracer-tracee ratio (TTR) [panel A] used to calculate whole-body production (WBP) of L-Phenylalanine [Ring-$^{13}C_6$)] (panel B) in low- and high-active mice over a period of 40 mins. Data are normalized for lean body mass (lbm) and expressed as mean (± 95% CI; panel A) and mean (± SE; panel B). Statistics are by t-test with alpha level set at $p \leq 0.05$.

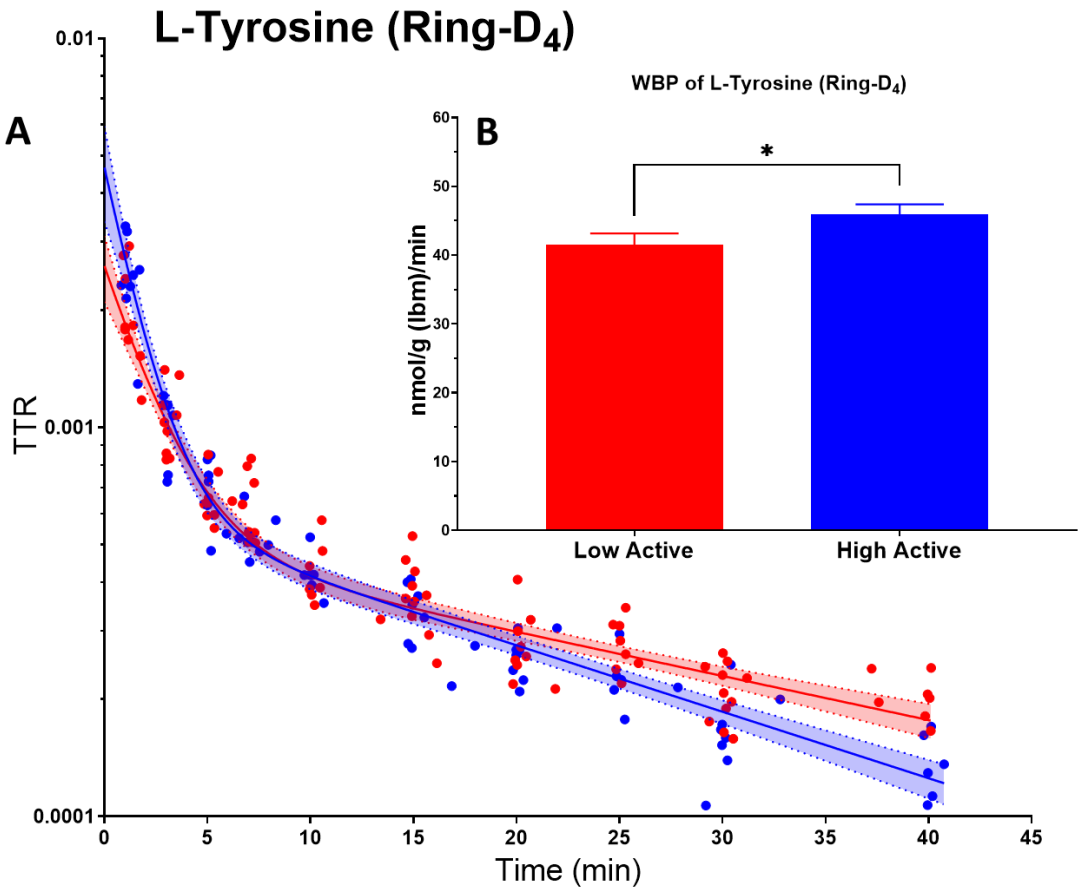

Figure 11 - Tyrosine TTR & Whole-Body Production: Logarithmic fitting of tracer-tracee ratio (TTR) [panel A] used to calculate whole-body production (WBP) of L-Tyrosine [Ring-D_4)] (panel B) in low- and high-active mice over a period of 40 mins. Data are normalized for lean body mass (lbm) and expressed as mean (± 95% CI; panel A) and mean (± SE; panel B). Statistics are by t-test with alpha level set at $p \leq 0.05$.

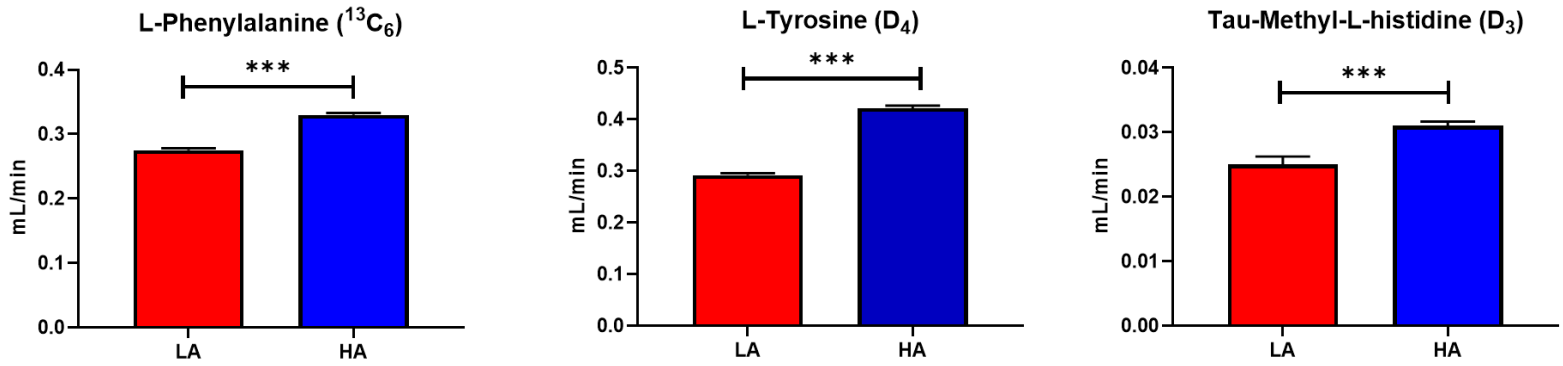

Figure 12 - Clearance Rates of Phenylalanine, Tyrosine, & Tau-Methyl-Histidine: Total clearance rate for L-phenylalanine ($^{13}C_6$), L-tyrosine (C_4), and tau-methyl-L-histidine (D_3) in low-active (red) and high-active (blue) mice over a period of 40 mins Clearance data was calculated as (whole-body production/plasma concentration) and expressed as mean (± SE). Statistics are by t-test, *** indicates $p \leq 0.001$.

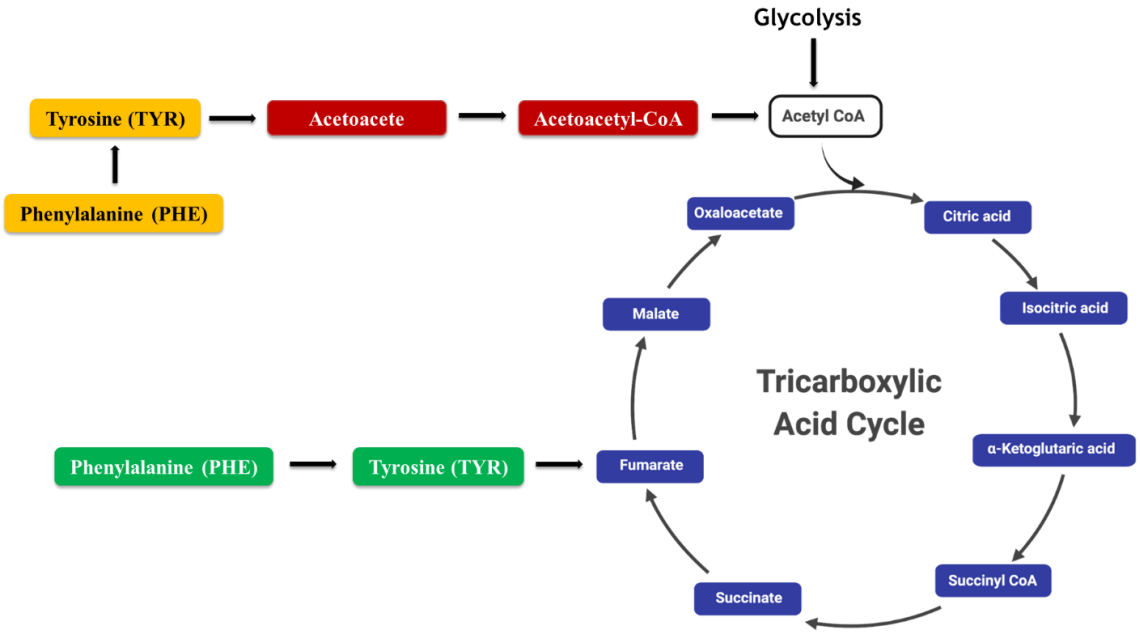

Figure 13 - Anaplerosis *via* Phenylalanine & Tyrosine: Overview of phenylalanine (PHE) and tyrosine (TYR) anaplerotic (replenishing) pathways of the TCA cycle. Green boxes represent PHE's and TYR's glucogenic pathway, while yellow depicts PHE's and TYR's ketogenic pathway.

APPENDIX B

TABLES

Table 1: Mouse Characteristics

Mouse Characteristics	LA: C3H/HeJ (n=23)	HA: C57L/J (n=20)	T-test (p)
Age (weeks)	12	12	-
Body Weight (g)	25.9 ± 0.3	27.5 ± 0.3	**<0.0001**
Lean Mass (g)	21.1 ± 0.2	22.5 ± 0.4	**0.0003**
Fat Mass (g)	2.6 ± 0.1	2.5 ± 0.1	0.5255
Free Body Water (g)	0.024 ± 0.005	0.018 ± 0.004	0.3398
Total Body Water (g)	1.79 ± 0.02	1.92 ± 0.03	**0.0006**
Bone Mineral Density (g/cm3)	0.059 ±0.004	0.057± 0.005	0.0713
Avg. Daily Food Consumption (g)	3.1 ± 0.2	3.4 ± 0.2	0.2482

Table 1: Data are mean (±SE) for low-active (LA) and high-active (HA) mice. Statistics are by t-test, bold indicates P<0.05

Table 2: Plasma Amino Acid Concentrations

Plasma Amino Acid Concentrations (µM)			
	LA: (n=23)	**HA: (n=20)**	**T-test (p)**
Glutamate	36.8 ± 2.9	17.5 ± 1.7	**<0.0001**
Glutamine	641.8 ± 23.9	633.7 ± 20.7	0.8011
Citrulline	57.3 ± 2.3	46.4 ± 1.5	**0.0003**
Arginine	104.6 ± 6.7	106.7 ± 4.2	0.7895
Ornithine	55.4 ± 7.3	36.9 ± 2.6	**0.0241**
Valine	187.9 ± 7.1	156.8 ± 4.9	**0.0008**
Isoleucine	57.7 ± 2.3	48.5 ± 1.9	**0.0041**
Leucine	144.8 ± 6.4	125.2 ± 4.8	0.0184
Phenylalanine	86.7 ± 4.3	77.5 ± 2.4	0.0724
Tyrosine	142.1 ± 5.6	108.7 ± 4.1	**<0.0001**
Tau-methylhistidine	8.0 ± 0.2	9.3 ± 0.3	**0.0011**

Data are mean ± (SE) in µM. Statistics are by t-test, bold is P<0.05.

Table 3: Composition of Stable Tracers in Bolus Pulse

Composition of stable tracers in bolus pulse

Isotopes	nmol/0.01 ml
L-Arginine:HCl (Guanidino-$^{15}N_2$)	381.7
L-Citrulline (5-^{13}C; 4,4,5,5-D_4)	137.2
L-Ornithine:HCL ($^{13}C_5$)	245.9
L-Glutamine ($^{15}N_2$)	1699.6
L-Glutamic acid (1,2-$^{13}C_2$)	196.8
L-Leucine ($^{13}C_6$)	474.4
L-Isoleucine (1-^{13}C)	395.4
L-Valine ($^{13}C_5$)	993.1
Tau-Methyl-L-histidine (Methyl-D_3)	38.2
L-Phenylalanine (Ring-$^{13}C_6$)	271.8
L-Tyrosine (Ring-D_4)	161.1